

**A luminescent *cis* iridium(III) complex based on a bis(6,7-dimethoxy-3,4-dihydroisoquinoline) platform featuring an unusual *cis* orientation of the C<sup>N</sup> ligands: from a theoretical approach to a deep red LEEC device**

Valeria Criscuolo,<sup>§</sup> Carmela T. Prontera,<sup>§</sup> Michele Pavone,<sup>§</sup> Orlando Crescenzi,<sup>§</sup> Maria G. Maglione,<sup>‡</sup> Paolo Tassini,<sup>‡</sup> Stefano Lettieri,<sup>†</sup> Pasqualino Maddalena,<sup>¶</sup> Carmela Borriello,<sup>‡</sup> Carla Minarini,<sup>‡</sup> Paola Manini<sup>§\*</sup>

<sup>§</sup> Department of Chemical Sciences, University of Naples Federico II, via Cintia 4, I-80126 Napoli, Italy

<sup>‡</sup> Laboratory of Nanomaterials and Devices (SSPT-PROMAS-NANO), ENEA – C. R. Portici, Piazzale Enrico Fermi 1, I-80055 Portici (NA), Italy

<sup>†</sup> Institute for Applied Sciences and Intelligent Systems “E. Caianiello” (CNR-ISASI), National Research Council, Via Campi Flegrei 34, Pozzuoli (NA), Italy

<sup>¶</sup> Department of Physics “E. Pancini”, University of Naples Federico II, via Cintia 4, I-80126 Napoli, Italy.

<b>Materials and methods</b>	<b>S2</b>
<b>Synthetic Procedures</b>	<b>S3-S4</b>
<b>NMR spectra</b>	<b>S5-S8</b>
<b>ESI-MS spectra (positive and negative ions) of <i>cis</i>-1</b>	<b>S9</b>
<b>Thermal behavior of <i>cis</i>-1</b>	<b>S10</b>
<b>Cyclic Voltammetry of <i>cis</i>-1</b>	<b>S11</b>
<b>Three-gaussian best-fit performed on the emission spectrum of <i>cis</i>-1</b>	<b>S12</b>
<b>PLE spectra of <i>cis</i>-1 at 9 K</b>	<b>S13</b>
<b>Schematic representation of the main opto-electronic transitions of <i>cis</i>-1</b>	<b>S14</b>
<b>Characteristics of the LEEC devices</b>	<b>S15-S18</b>
<b>Computational investigation</b>	<b>S19-S43</b>
<b>References</b>	<b>S44-S46</b>

## **Materials and methods**

All reactants and solvents, unless otherwise stated, were purchased from commercial sources and used as received.

$^1\text{H}$ ,  $^{13}\text{C}$  and  $^{19}\text{F}$  spectra were acquired on a Bruker DRX (400 MHz) spectrometer.

Chemical shifts are given in ppm relative to the internal standard tetramethylsilane ( $\text{Me}_4\text{Si}$ ) and  $J$  values are given in Hz.  $^1\text{H}, ^1\text{H}$  COSY,  $^1\text{H}, ^{13}\text{C}$  HSQC,  $^1\text{H}, ^{13}\text{C}$  HMBC and NOESY experiments were run at 400.1 MHz using standard pulse programs. Mass spectra were recorded in positive and negative ion mode using a 1100 VL LC/MSD Agilent instrument.

Absorption and photoluminescent (PL) spectra were recorded with a UV-vis spectrophotometer (Jasco V-560) and a fluorospectrophotometer (Jasco FP-750).

Quantum efficiencies ( $\Phi$ ) were calculated using fluorescein ( $\Phi = 0.9$  in a 0.1 M solution of NaOH) as reference.

Analytical and preparative TLC were performed on silica gel plates F254 (0.25 and 0.5 mm, respectively) and were visualized using a UV lamp ( $\lambda = 254$  nm) and a fluorescence lamp ( $\lambda = 356$  nm). Liquid chromatography was performed on silica gel (60-230 mesh).

The cyclic voltammetry (CV) measurements were performed using a potentiostat/galvanostat model 273A (Princeton Applied Research). Ag/AgCl reference electrode, Pt tip electrode (0.008 mm<sup>2</sup>

area), and Pt counter electrode were used. For CV measurements, we used an electrolytic solution having standard concentration of 0.1 M di tetrabutylammonium hexafluorophosphate and a scan rate of 50 and 100 mV/s. The system has been previously tested and calibrated using a ferrocene solution in acetonitrile (0.02 M).

The thickness of films was determined with an Taylor Hobson CCI MP profilometer.

## Synthetic Procedures

**Synthesis of bis(6,7-dimethoxy-3,4-dihydroisoquinoline).** A reported procedure for the synthesis of the ancillary ligand was followed.<sup>1</sup> In brief, a solution of diethyloxalate (3.66 mL, 27 mmol) in toluene (9 mL) was added to a solution of *O,O*-dimethyldopamine (1 g, 5.9 mmol) in toluene (50 mL). The mixture was heated to reflux under argon for 5 h and then evaporated under reduced pressure. The crude solid was taken in chloroform and purified by liquid chromatography on silica gel using chloroform as the eluent to give the N1,N2-bis(3,4-dimethoxyphenethyl)oxalamide (1.17 g, 95%, R<sub>f</sub> = 0.78 chloroform/methanol 95:5 (v/v)).

<sup>1</sup>H NMR (200 MHz, Acetone-d<sub>6</sub>) δ ppm: 6.86 (d, *J* = 2.0 Hz, 1H), 6.82 (d, *J* = 6.2 Hz, 1H), 6.76 (dd, *J* = 6.2, 2.0 Hz, 1H), 3.79 (s, 3H), 3.77 (s, 3H), 3.49 (t, *J* = 4.0 Hz, 2H), 2.83 (t, *J* = 4.0 Hz, 2H).

<sup>13</sup>C NMR (50 MHz, acetone-d<sub>6</sub>) δ ppm: 158.7, 150.2, 148.9, 132.3, 121.3, 113.4, 112.7, 63.2, 62.8, 55.9, 41.6.

A solution of the N1,N2-bis(3,4-dimethoxyphenethyl)oxalamide (1.17 g, 2.8 mmol) in 11 mL of a mixture 3:11 (v/v) of ethanol/dichloromethane was treated under stirring with

POCl<sub>3</sub> (3.7 mL, 39 mmol) and kept under reflux. After 5 h, 8.9 mL of light petroleum were added and the mixture was kept at 130 °C overnight. The mixture was filtered and the solid was dissolved in water/methanol (1.7 mL / 50 mL) and treated with K<sub>2</sub>CO<sub>3</sub> (350 mg) to adjust the pH to 10 and then extracted with chloroform. The crude solid was purified by liquid chromatography on silica gel using chloroform as eluent to give the pure bis(6,7-dimethoxy-3,4-dihydroisoquinoline) (650 mg, 61%, R<sub>f</sub>= 0.75, chloroform/methanol 95:5 (v/v)). <sup>1</sup>H NMR (400 MHz, CDCl<sub>3</sub>) δ ppm: 7.24 (s, 1H), 6.57 (s, 1H), 3.78 (s, 3H), 3.75 (s, 3H), 3.71 (t, J= 7.6 Hz, 2H), 2.56 (t, J= 7.6, 2H). <sup>13</sup>C NMR (50 MHz, CDCl<sub>3</sub>) δ ppm: 164.4, 151.3, 147.1, 131.2, 118.5, 110.0, 109.8, 55.7, 55.5, 47.2, 24.7. ESI<sup>+</sup> MS: *m/z* 381.

**Synthesis of [Ir(ppy)<sub>2</sub>Cl]<sub>2</sub>.** For the synthesis of the dichloro-bridged iridium complex was followed the procedure reported by Nonoyama.<sup>2</sup> In brief, iridium trichloride hydrate (500 mg, 1.67 mmol) was dissolved in a mixture of 32 mL of 2-ethoxyethanol and water 3:1 (v/v) and treated with 480 μL (3.6 mmol) of 2-phenylpyridine under reflux and argon atmosphere. After 24 h the reaction mixture was cooled and filtered on a glass filter frit to obtain a yellow precipitate (644 mg, 72%).

<sup>1</sup>H NMR (400 MHz, CD<sub>2</sub>Cl<sub>2</sub>) δ ppm: 9.30 (d, *J* = 8.0 Hz, 2H), 7.98 (d, *J* = 8.0 Hz, 2H), 7.84 (t, *J* = 8.0 Hz, 2H), 7.60 (d, *J* = 8.0 Hz, 2H), 6.8-6.9 (m, 4H), 6.65 (t, *J* = 8.0 Hz, 2H), 5.92 (d, *J* = 8.0 Hz, 2H).

**Figure S1.**  $^1\text{H}$  NMR spectrum of *cis*-1 ( $\text{CD}_2\text{Cl}_2$ )

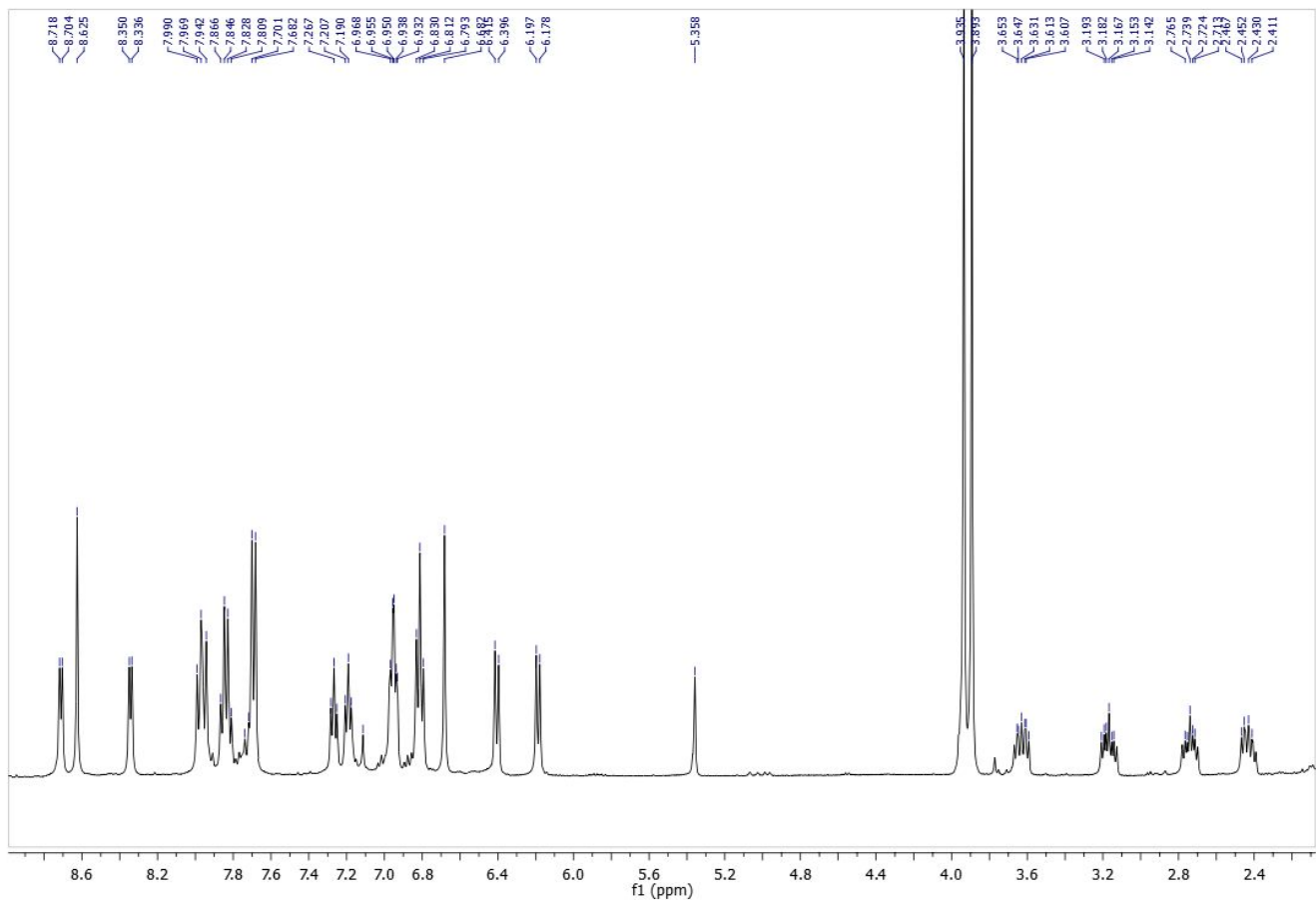


**Figure S2.**  $^1\text{H}$  NMR spectrum of *cis*-5 (CD<sub>2</sub>Cl<sub>2</sub>)

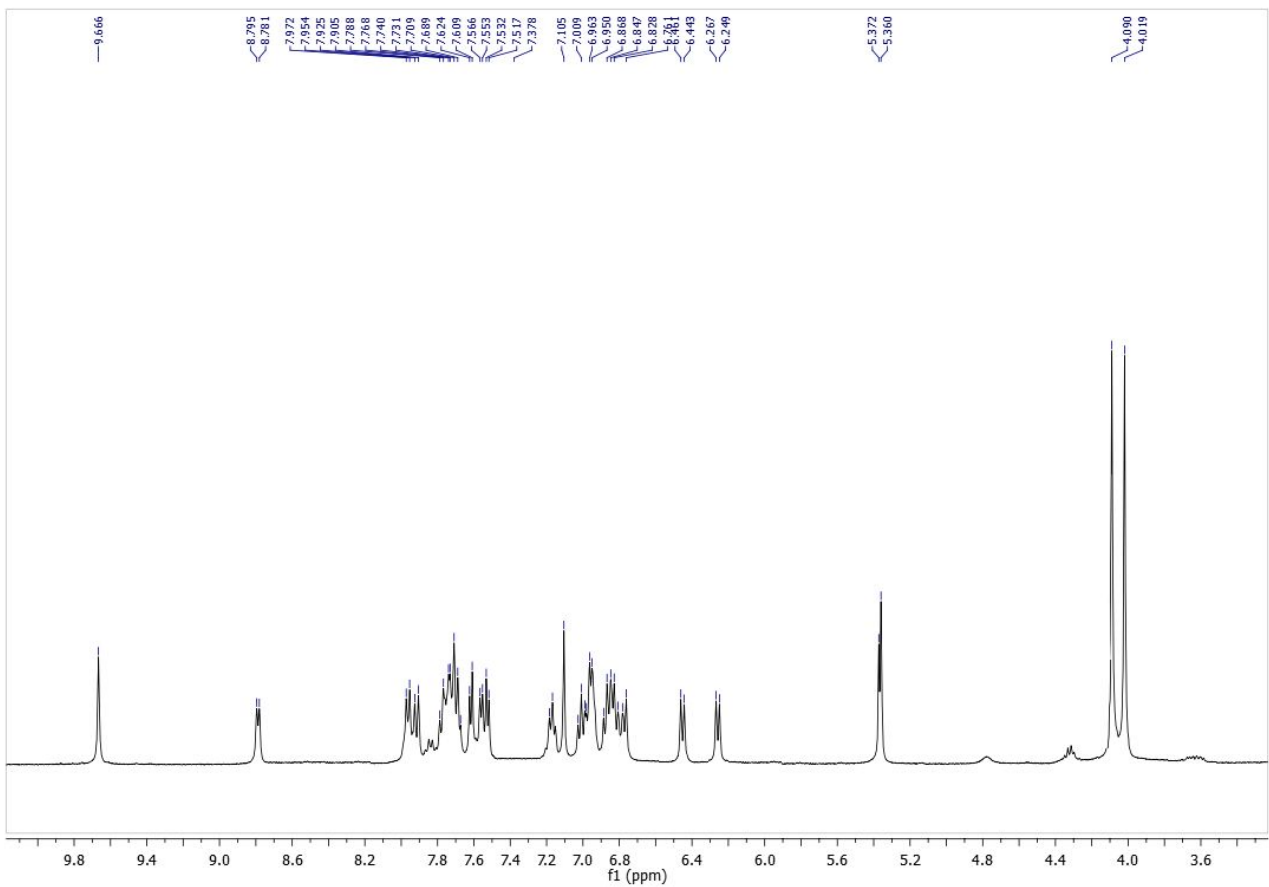
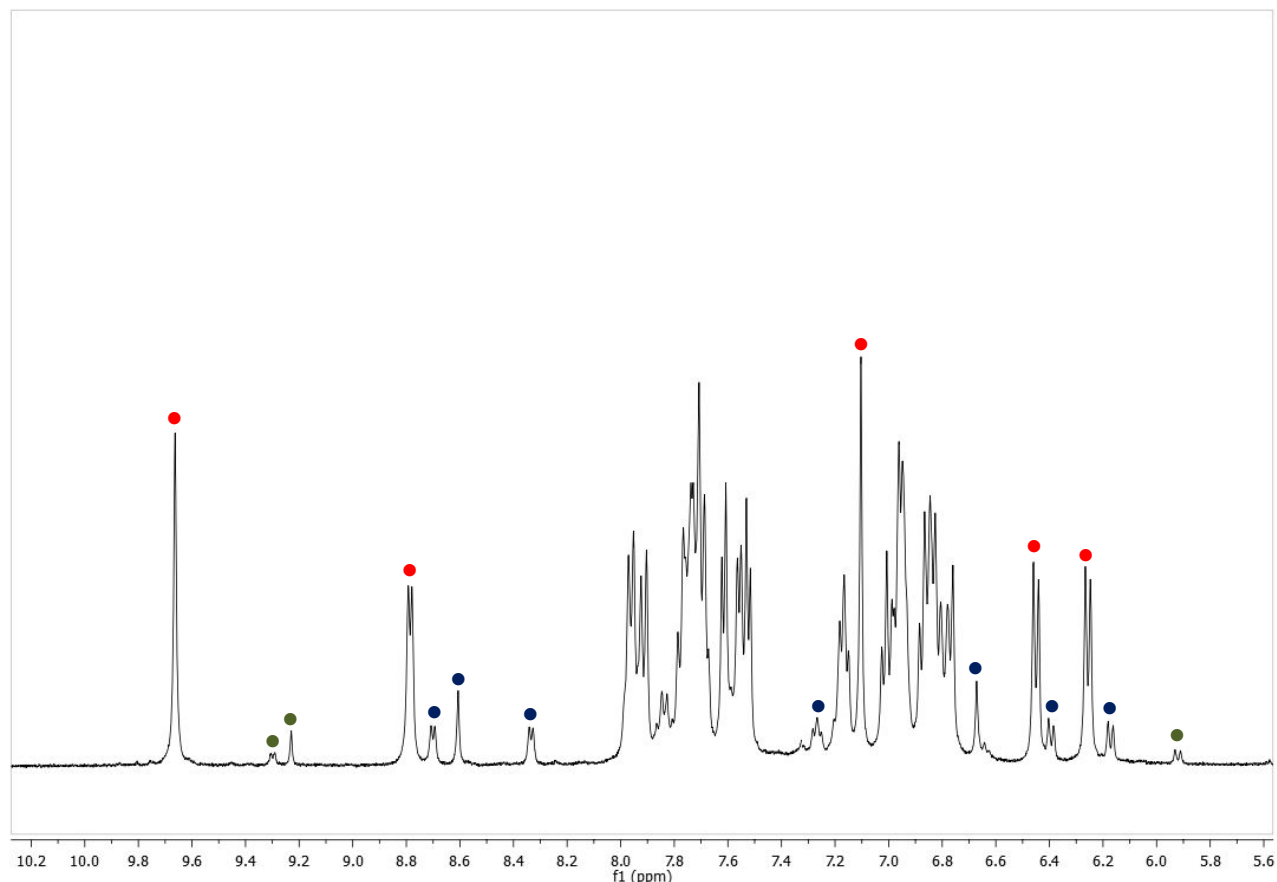


**Figure S3.**  $^1\text{H}$  NMR spectrum ( $\text{CD}_2\text{Cl}_2$ , expansion of the aromatic protons region) of a *cis*-**5** enriched fraction obtained from liquid chromatography of the reaction mixture for iridium(III) complex preparation.



- signals diagnostic of *cis*-**5**
- signals diagnostic of *cis*-**1**
- signals diagnostic of *trans*-**1**

**Figure S4.**  $^1\text{H},^1\text{H}$  COSY spectrum ( $\text{CD}_2\text{Cl}_2$ , expansion of the aromatic protons region) of a *cis*-5 enriched fraction obtained from liquid chromatography of the reaction mixture for iridium(III) complex preparation.

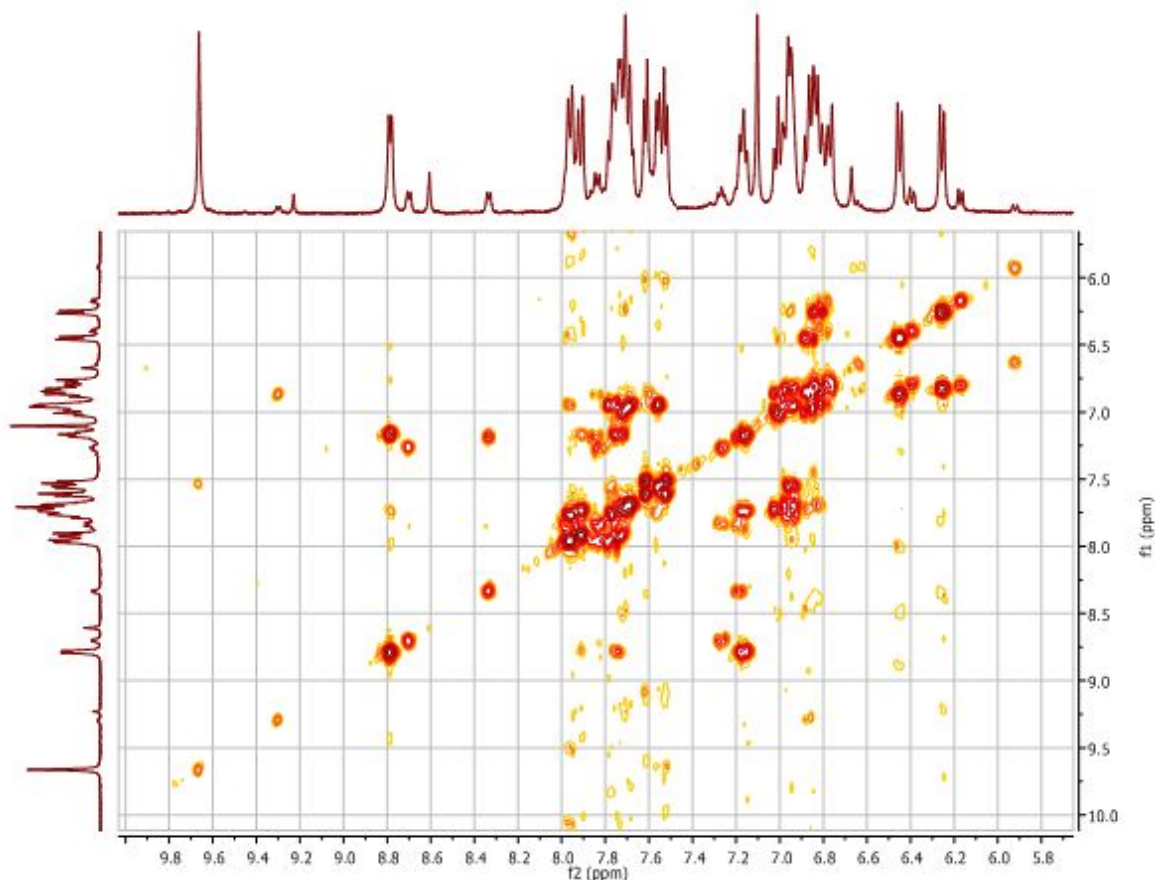
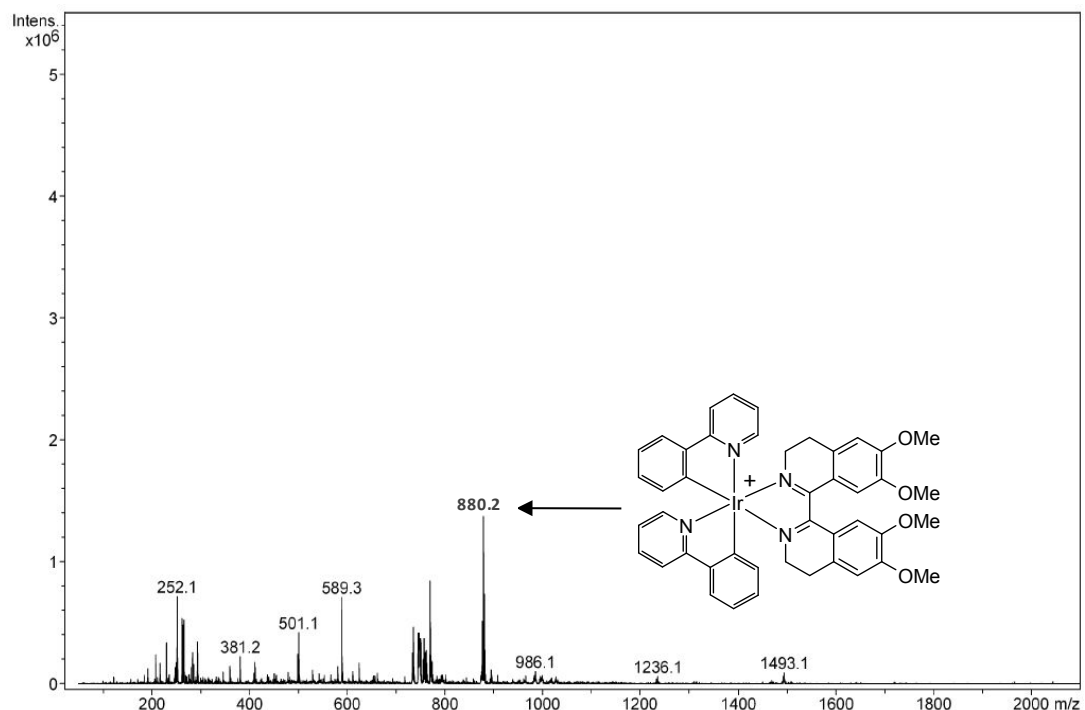


**Figure S5. (a) ESI(+)–MS spectrum of *cis*-1; (b) ESI(–)-MS spectrum of *cis*-1**

(a)



(b)

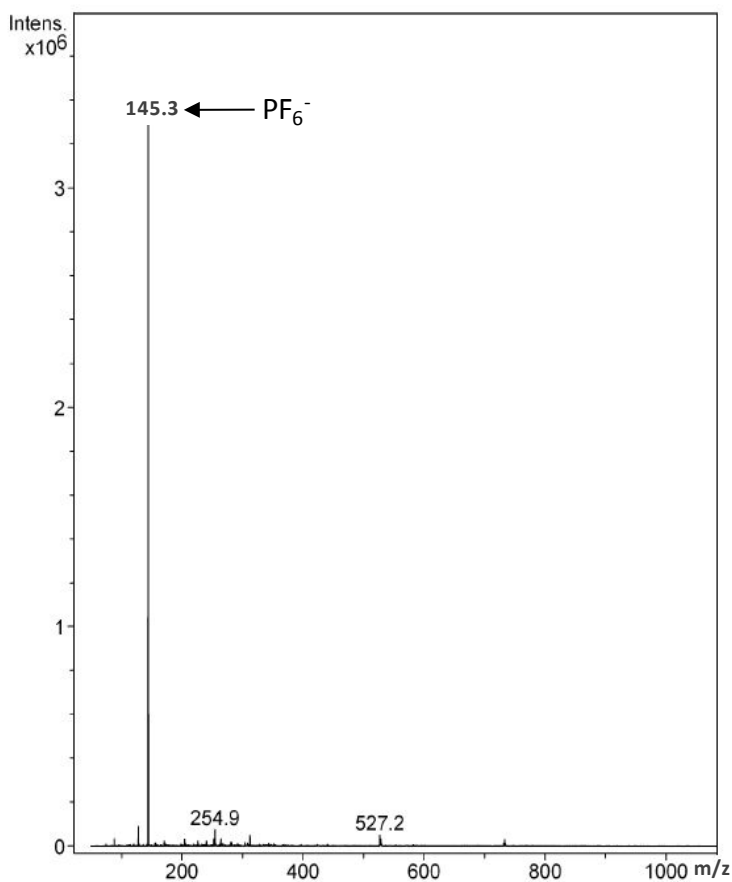
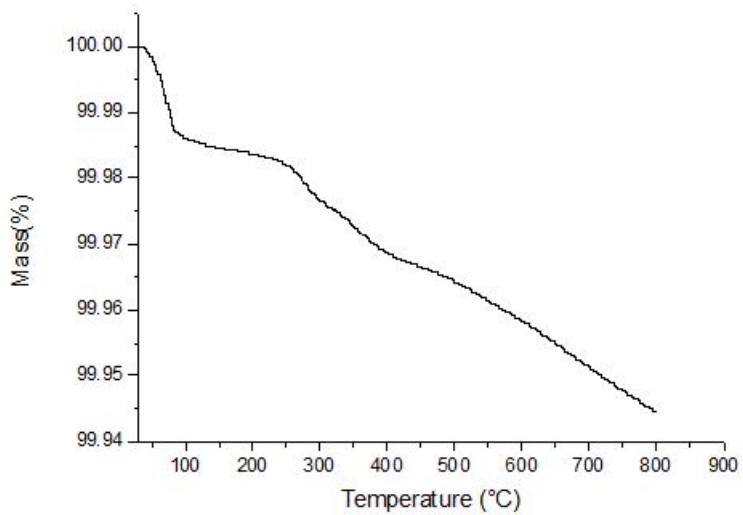


**Figure S6. (a) Thermo Gravimetric Analysis (TGA) of *cis*-1; (b) Differential Scanning Calorimetry (DSC) of *cis*-1**

(a)



(b)

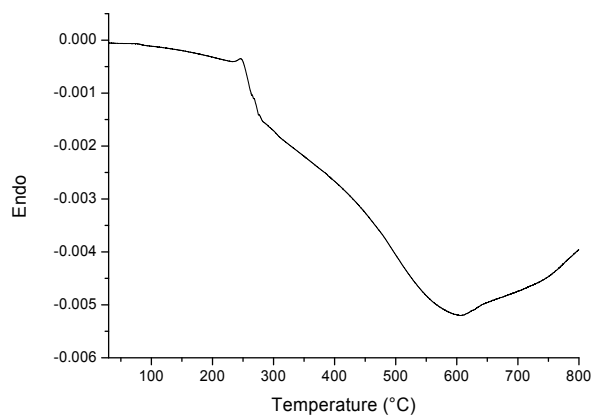


**Figure S7.** Cyclic voltammogram of *cis*-**1** (scan rate = 50 mVs<sup>-1</sup>).

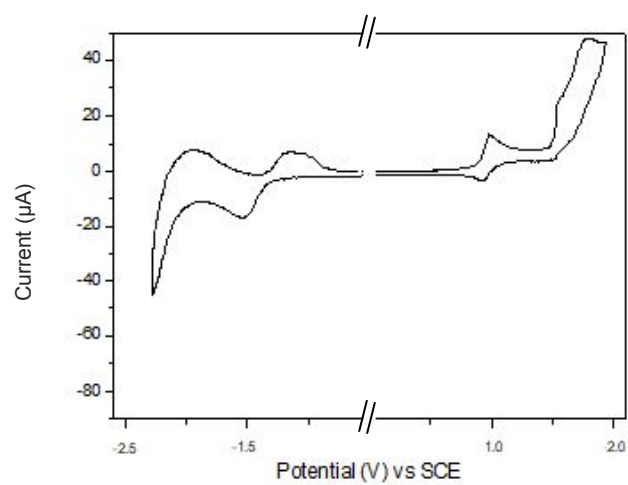


**Figure S8.** Three-gaussian best-fit performed on the emission spectrum of *cis*-**1**. Experimental emission spectrum registered at 9 K after excitation at 440 nm (bold black line); fitted curve (regular black line); extrapolated single spectral contributions at 2.08 eV (blue line), 1.93 eV (green line) and 1.71 eV (red line).

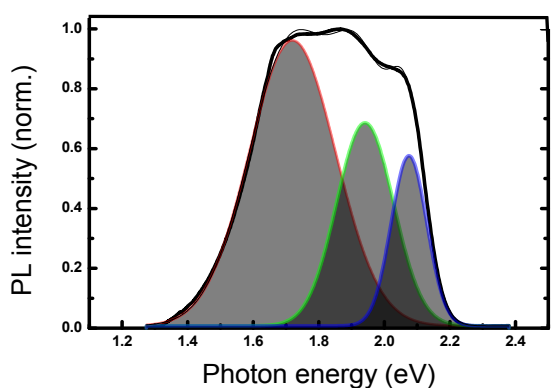


**Figure S9.** Normalized PLE spectra obtained at 9 K of the three emission bands E1 (white circle), E2 (yellow square) and E3 (blue circle) of *cis*-1.

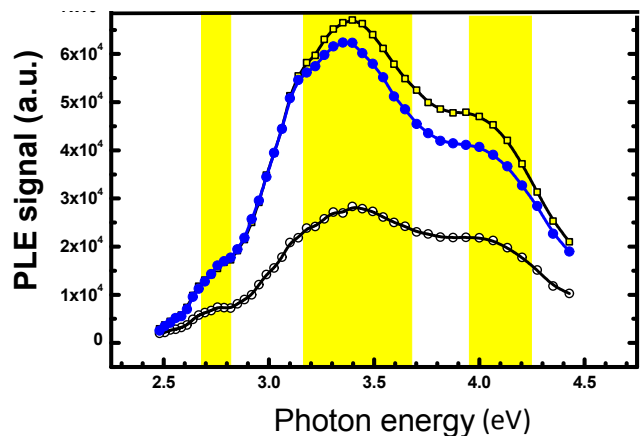


**Figure S10.**Schematic representation of the main opto-electronic transitions of *cis*-**1**. Spin-forbidden transitions are highlighted in red.

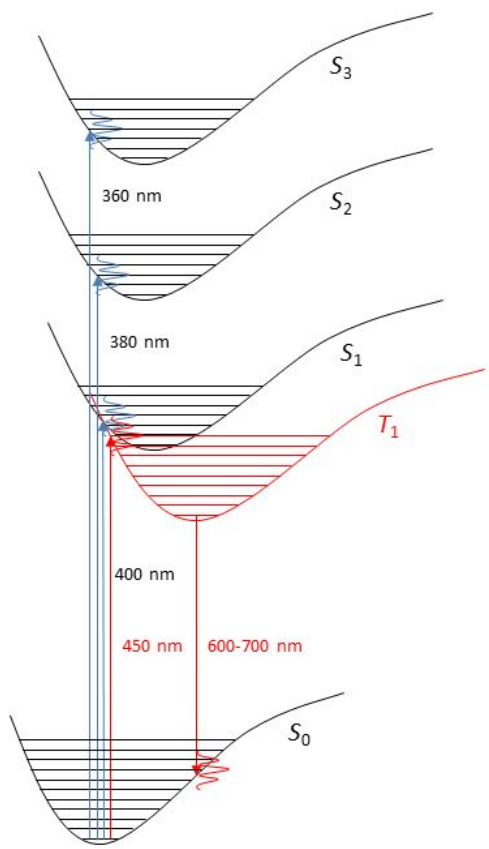


**Figure S11. Characteristic of the LEEC devices #4, #6 and #8**

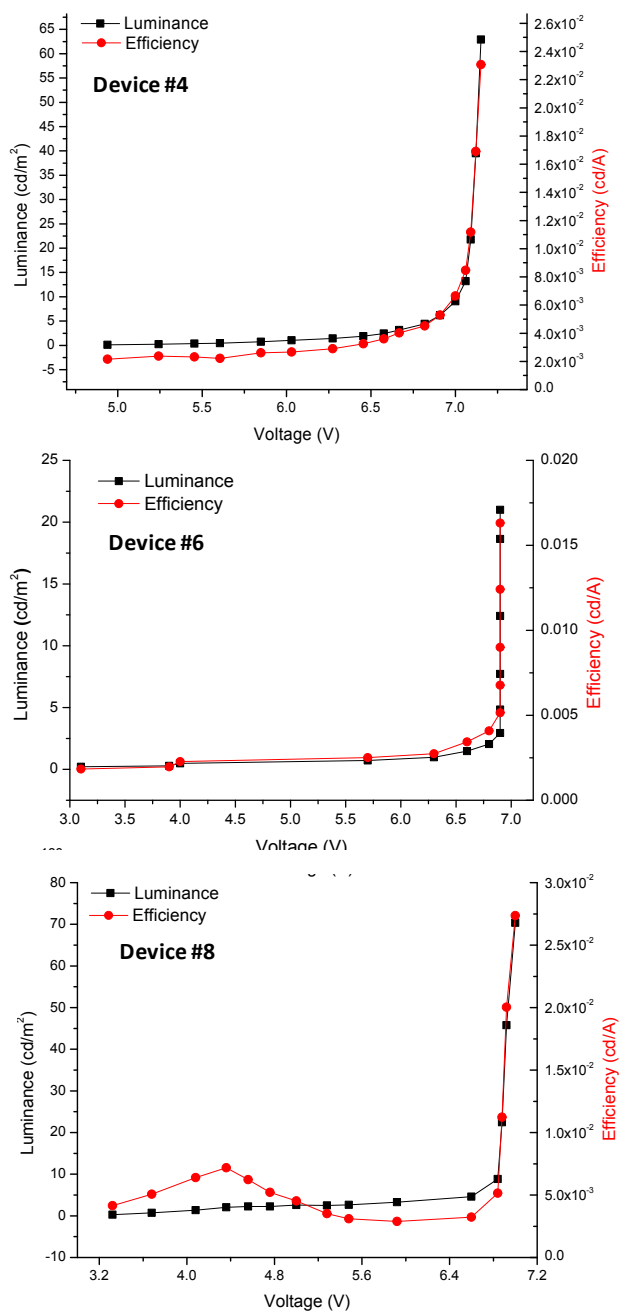
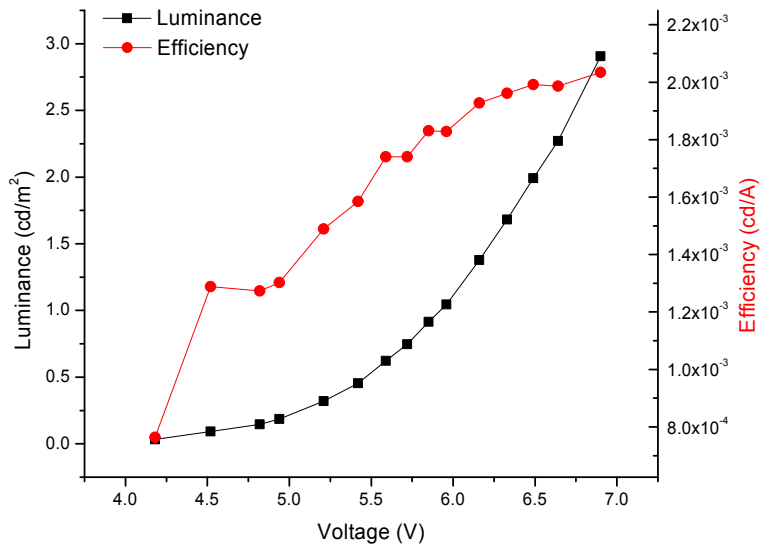
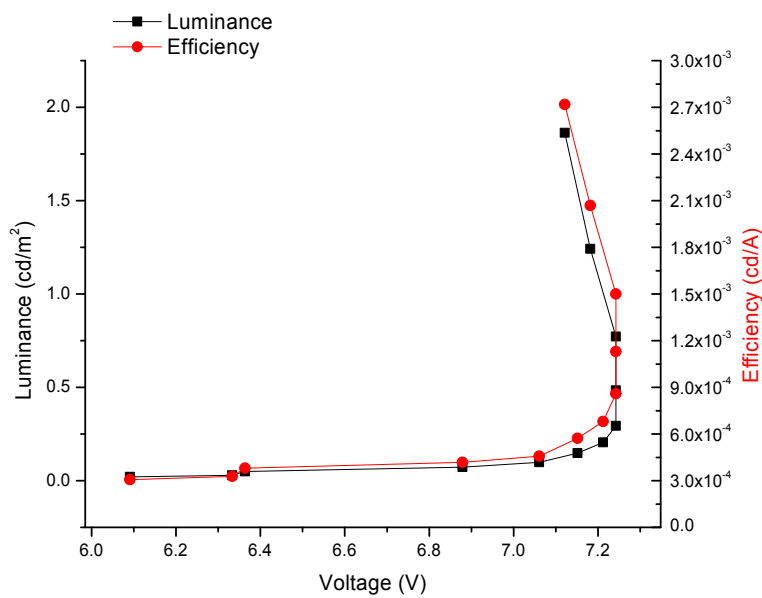


**Figure S12. Characteristic of the following LEEC devices: (a) #1; (b) #2; (c) #3; (d) #5**

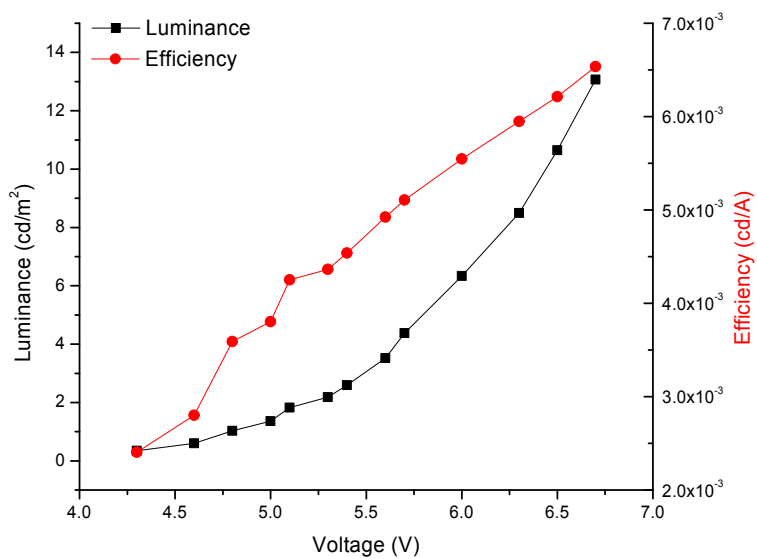
(a)



(b)



(c)



(d)

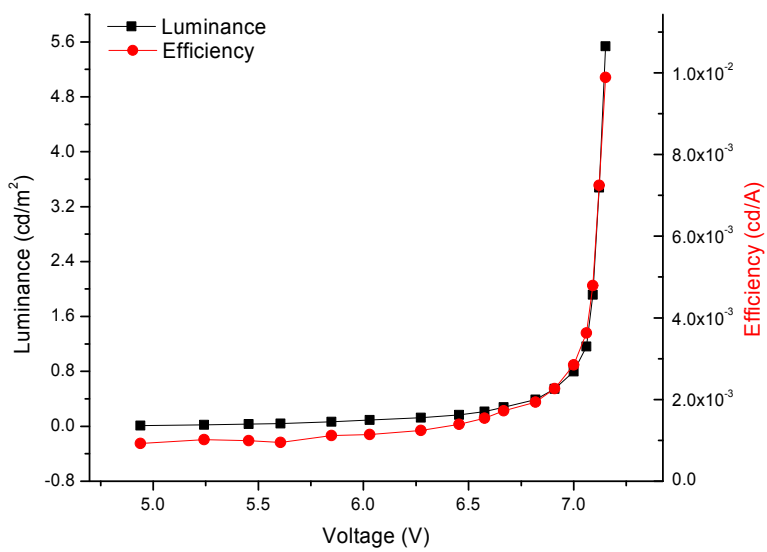
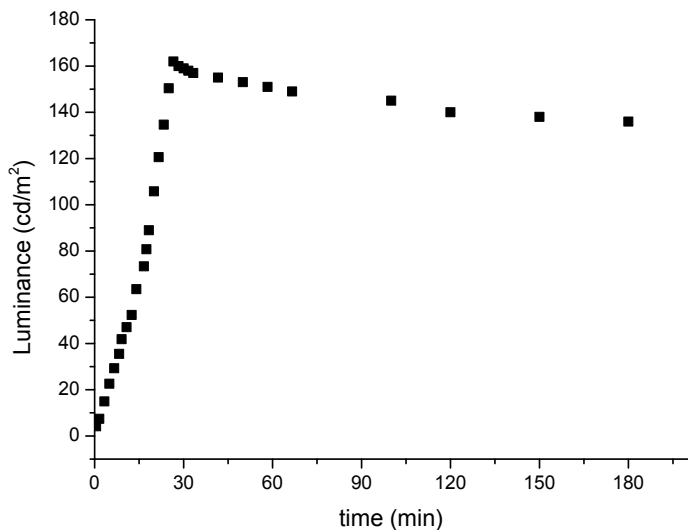
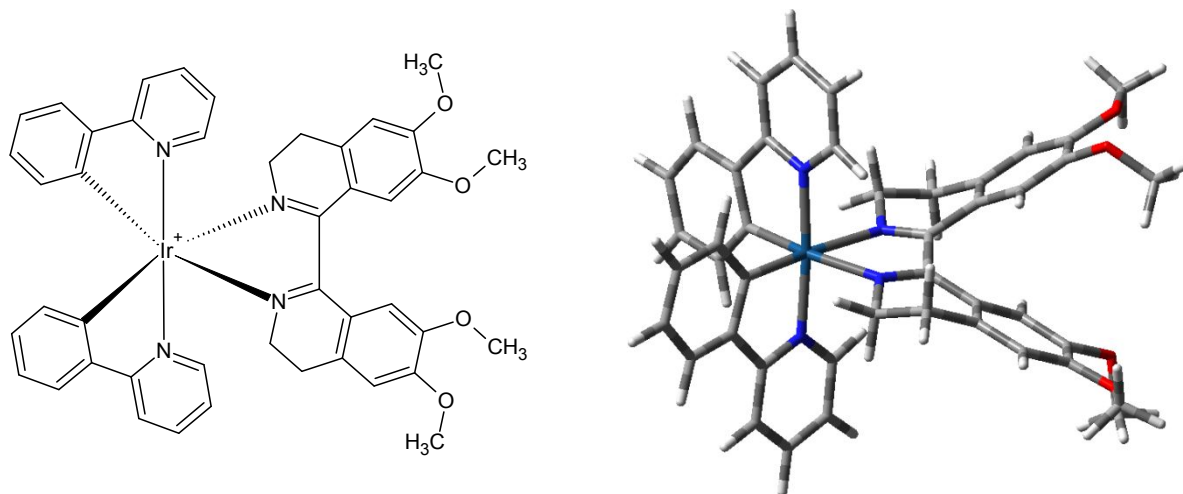


**Figure S13. Time-dependence of luminance for the best performing device #7**



## Computational investigation of structural and spectroscopic properties of iridium complexes

The aim of this investigation is to characterize structural, energetic and spectroscopic features of iridium complexes of 3,3',4,4'-tetrahydro-6,6',7,7'-tetramethoxy-1,1'-biisoquinoline, e.g.:



All calculations were performed with the Gaussian package of programs.<sup>3</sup>

All structures were geometry optimized at the DFT level with a hybrid functional (M06-2X).<sup>4</sup> The 6-31+G(d,p) basis set was used of H, C, N and O atoms; the Stuttgart / Dresden pseudopotential and basis set<sup>5,6</sup> were adopted for the iridium center. For each species, different conformers were explored. In those cases where conformational enantiomers exist, a single enantiomeric series has been examined.

To account for the influence of the solution environment (chloroform), a polarizable continuum medium (PCM) was adopted.<sup>7-10</sup> In view of the faster convergence, a scaled van der Waals cavity based on universal force field (UFF) radii<sup>11</sup> was used, and polarization charges were modeled by spherical Gaussian functions.<sup>12,13</sup> Vibrational-rotational contributions to the free energy were also computed.

UV-Vis spectra of the main species were computed in solution using the time-dependent density functional theory (TD-DFT) approach,<sup>14-18</sup> with the same functional / basis set / pseudopotential combination. For the purpose of comparison, selected TD-DFT calculations were also performed using the PBE0,<sup>19</sup> CAM-B3LYP<sup>20</sup> or the LC- $\omega$ PBE<sup>21</sup> functional. To produce graphs, transitions below 5.6 eV were selected, and an arbitrary Gaussian line width of 0.25 eV was imposed; the spectra were finally converted to a wavelength scale. The non-equilibrium linear response formulation of the PCM was adopted for TD-DFT calculations; a state-specific approach<sup>22,23</sup> was employed to evaluate the energy of the first triplet state at the equilibrium geometry of the ground-state singlet, or vice-versa the energy of the ground-state singlet at the equilibrium geometry of the first triplet.

## Part 1: Parent compound

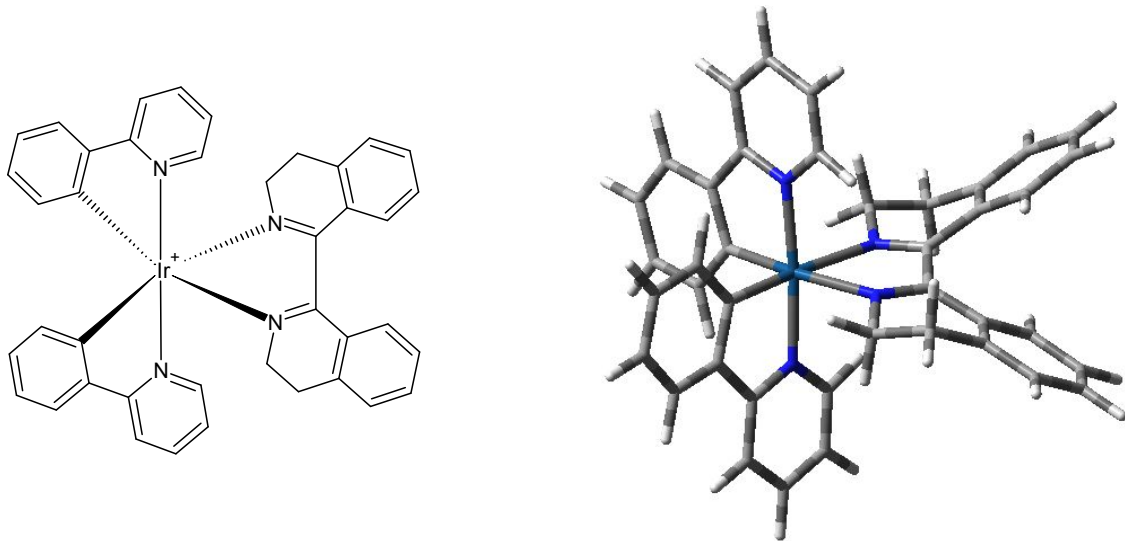


**Table S1.** Structural exploration of alternative isomers / conformers of the parent compound (monocation, singlet). In parentheses relative energies (kcal mol<sup>-1</sup>) referred to the most stable form (in bold) identified at the specified level.

#	Isomer / Conformer <sup>a</sup>	Symmetry	$E_{PCM}$ / Ha <sup>b</sup>	$H_{PCM,RRHO}$ / Ha	$G_{PCM,RRHO}$ / Ha
apical_apical/.../conf1.symm	apical, apical, conf1	$C_2$	- <b>1866.096748 (0.0)</b>	- <b>1865.433334 (0.0)</b>	- <b>1865.535933 (0.0)</b>
apical_apical/.../conf2.symm	apical, apical, conf2	$C_2$	- 1866.094055 (1.7)	- 1865.430581 (1.7)	- 1865.532849 (1.9)
apical_equatorial/.../conf1	apical, equatorial, conf1	$C_1$	- 1866.094816 (1.2)	- 1865.431159 (1.4)	- 1865.534975 (0.6)
apical_equatorial/.../conf2	apical, equatorial, conf2	$C_1$	- 1866.093616 (2.0)	- 1865.430020 (2.1)	- 1865.535887 (0.0)
equatorial_equatorial/.../conf1.sym	equatorial, equatorial,	$C_2$	- 1866.07920	- 1865.41585	- 1865.52104

m	conf1		0 (11.0)	6 (11.0)	9 (9.3)
equatorial_equatorial/.../conf2.sym m	equatorial, equatorial, conf2	$C_2$	- 1866.07964 8 (10.7)	- 1865.41591 4 (10.9)	- 1865.51763 5 (11.5)

[a] For chiral structures, only one enantiomer is listed.

[b] Electronic energy.

**Figure S14.** UV-Vis spectra computed at the TD-M062X level for several isomers / conformers of the parent compound (monocation, singlet).

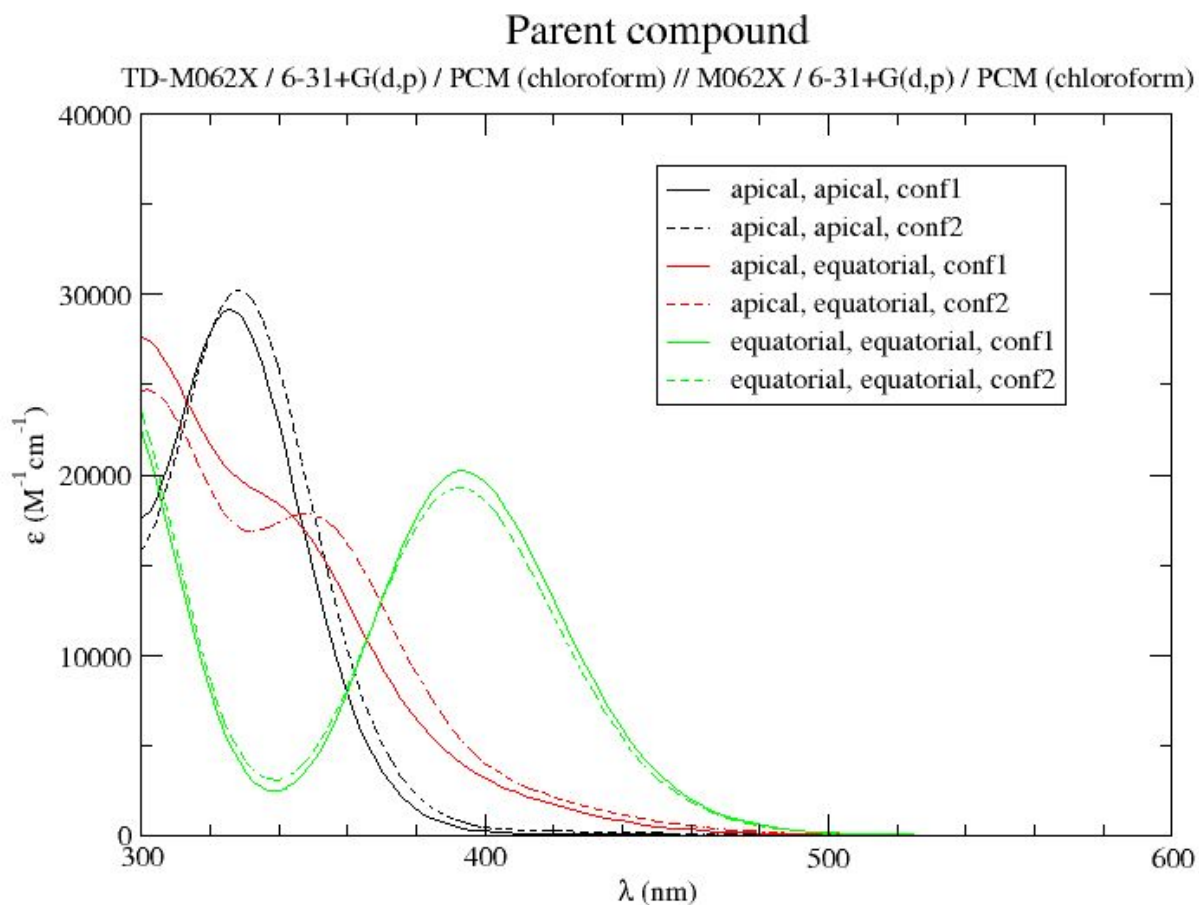
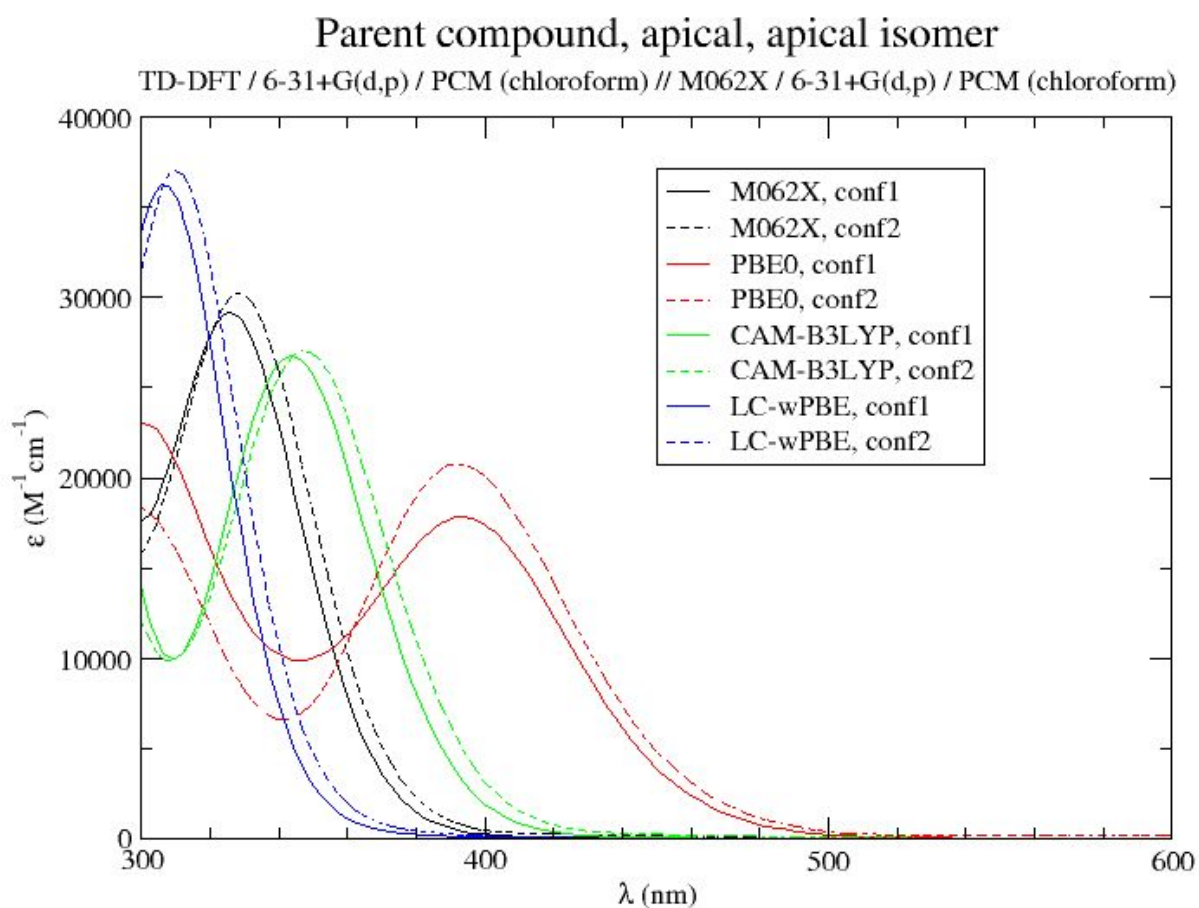


**Figure S15.** UV-Vis spectra computed with several different functionals, for two conformers of the apical, apical isomer of the parent compound (monocation, singlet).



## Part 2: Model 1

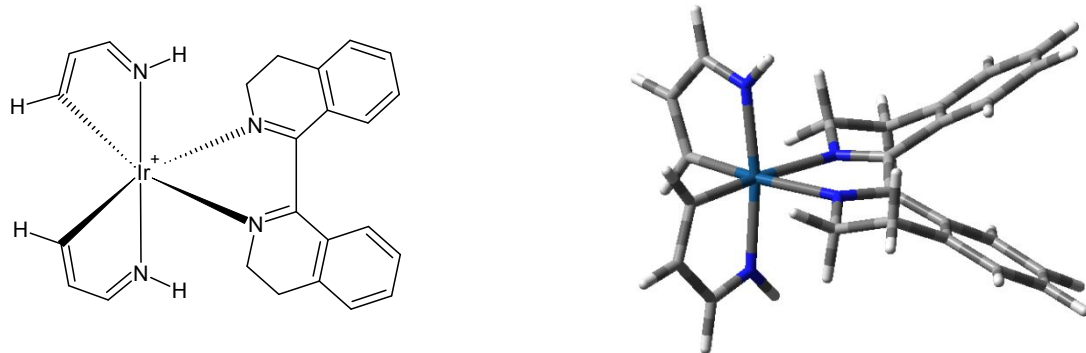


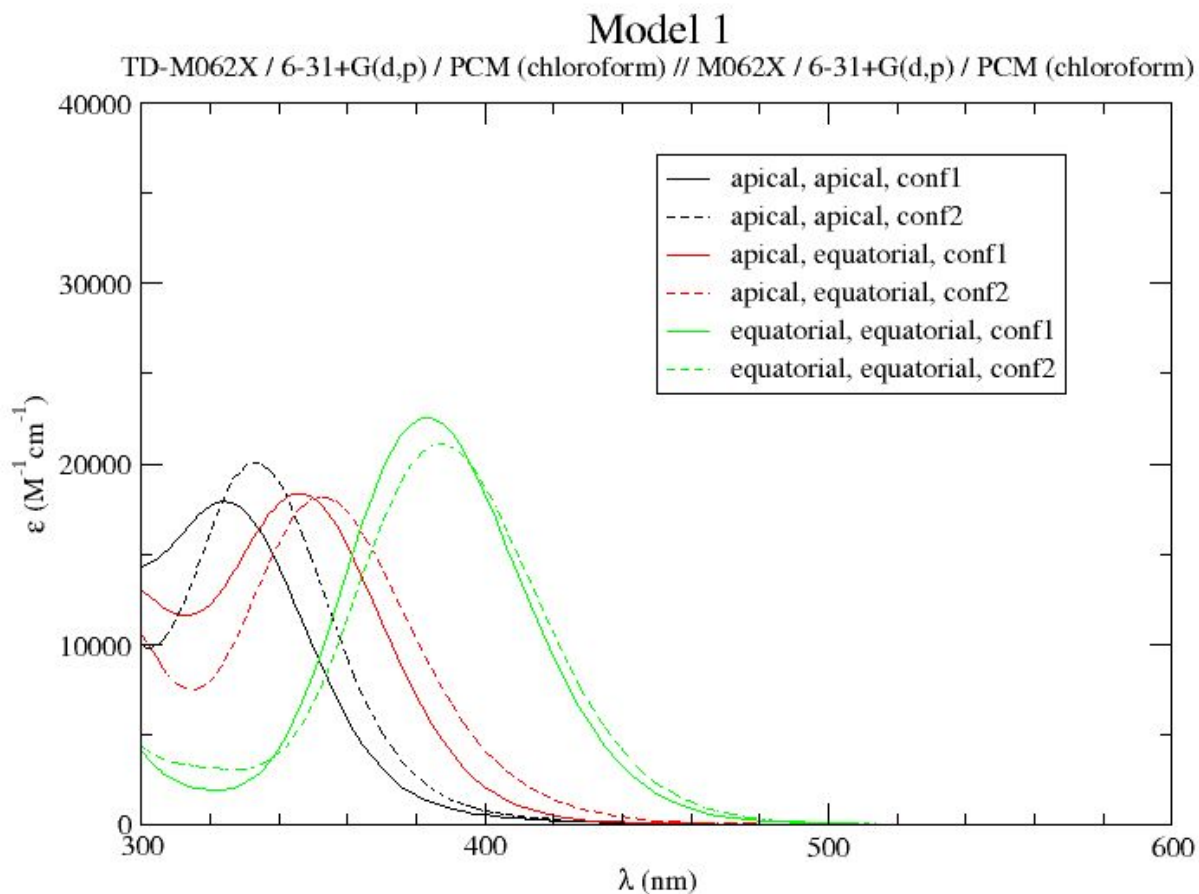
**Table S2.** Structural exploration of alternative isomers / conformers of model 1 (monocation, singlet). In parentheses relative energies (kcal mol<sup>-1</sup>) referred to the most stable form (in bold) identified at the specified level.

#	Isomer / Conformer <sup>a</sup>	Symmetry	$E_{\text{PCM}} / \text{Ha}^{\text{b}}$	$H_{\text{PCM,RRHO}} / \text{Ha}$	$G_{\text{PCM,RRHO}} / \text{Ha}$
apical_apical/.../conf1.symm	apical, apical, conf1	$C_2$	- <b>1251.69603 2 (0.0)</b>	- 1251.23241 2 (0.0)	- 1251.31064 8 (0.2)
apical_apical/.../conf2.symm	apical, apical, conf2	$C_2$	- 1251.69577 0 (0.2)	- <b>1251.23246 2 (0.0)</b>	- <b>1251.31097 3 (0.0)</b>
apical_apical/.../conf1	apical, equatorial, conf1	$C_1$	- 1251.69344 8 (1.6)	- 1251.23015 0 (1.5)	- 1251.30926 9 (1.1)
apical_apical/.../conf2	apical, equatorial, conf2	$C_1$	- 1251.69359 2 (1.5)	- 1251.23054 7 (1.2)	- 1251.31011 2 (0.5)
equatorial_equatorial/.../conf1.symm	apical, apical, conf1	$C_2$	- 1251.67804 0 (11.3)	- 1251.21459 8 (11.2)	- 1251.29188 6 (12.0)
equatorial_equatorial/.../conf2.symm	apical, apical, conf2	$C_2$	- 1251.67836 2 (11.1)	- 1251.21526 2 (10.8)	- 1251.29317 1 (11.2)

[a] For chiral structures, only one enantiomer is listed.

[b] Electronic energy.

**Figure S16.** UV-Vis spectra computed at the TD-M062X level for several isomers / conformers of model 1 (monocation, singlet).



### Part 3: Model 2

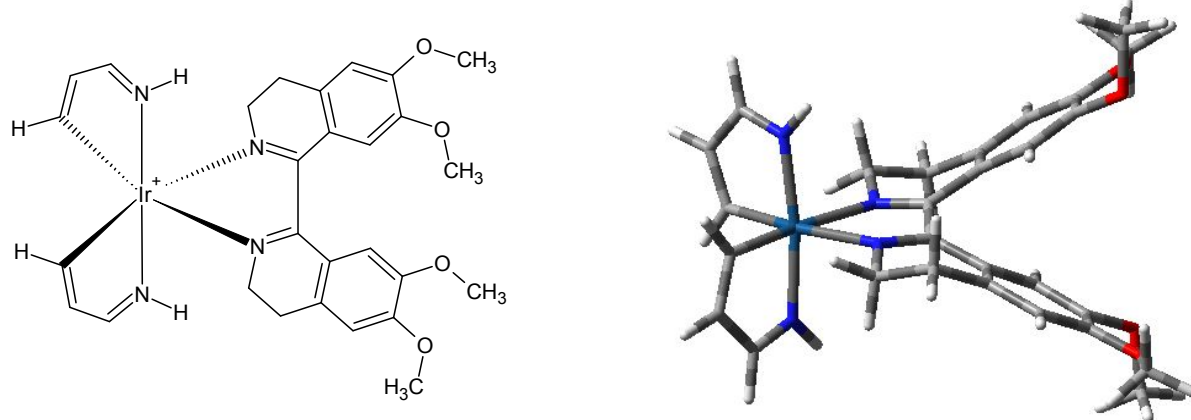


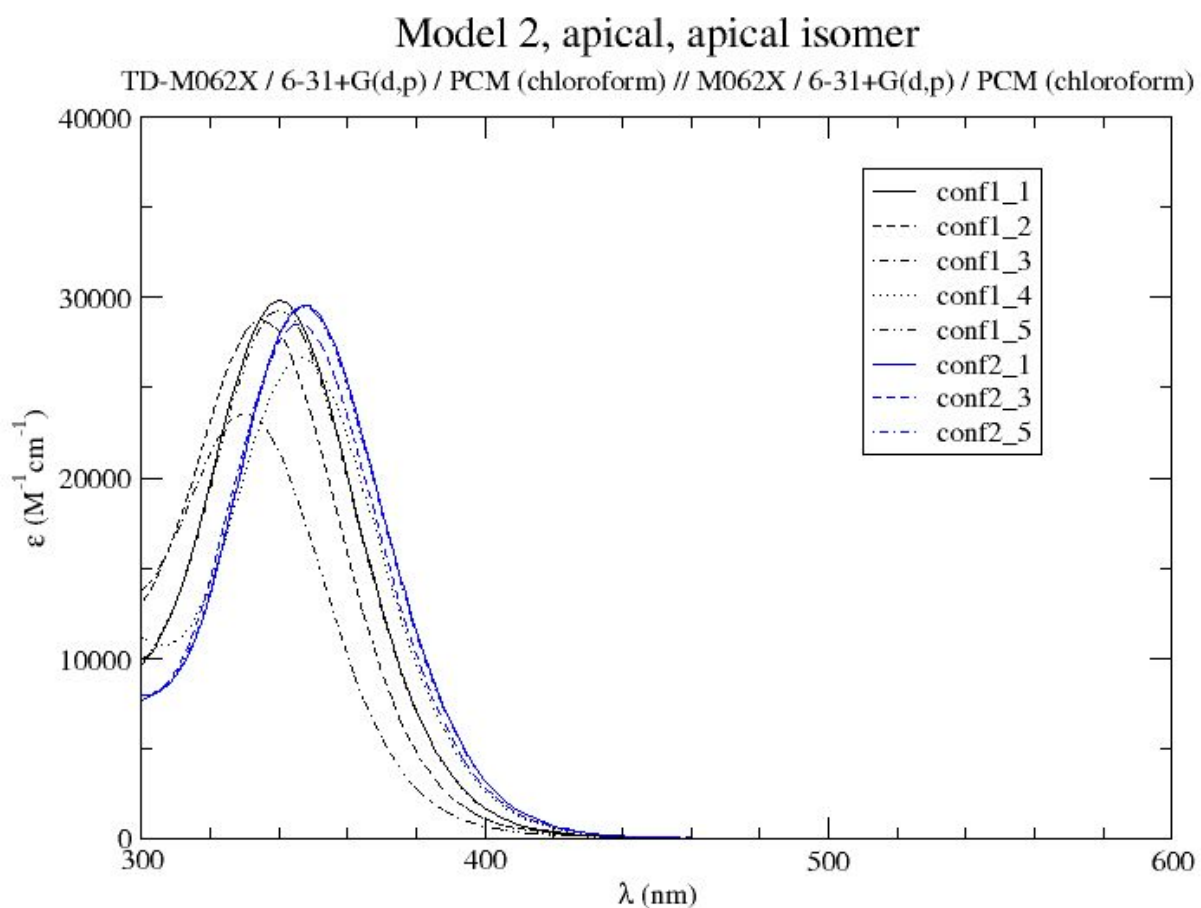
**Table S3.** Structural exploration of alternative conformers of the apical, apical isomer of model 2 (monocation, singlet). In parentheses relative energies (kcal mol<sup>-1</sup>) referred to the most stable form (in bold) identified at the specified level.

#	Isomer / Conformer <sup>a</sup>	Symmetry	$E_{PCM} / \text{Ha}^b$	$H_{PCM,RRHO} / \text{Ha}$	$G_{PCM,RRHO} / \text{Ha}$
apical_apical/.../conf1_1.symm	apical, apical, conf1_1	$C_2$	-1709.619821 (0.8)	-1709.014232 (0.8)	-1709.117151 (1.4)
apical_apical/.../conf1_2.symm	apical, apical, conf1_2	$C_2$	-1709.611761 (5.9)	-1709.006734 (5.5)	-1709.112059 (4.6)
apical_apical/.../conf1_3.symm	apical, apical, conf1_1	$C_2$	-1709.610939 (6.4)	-1709.005565 (6.2)	-1709.108790 (6.7)
apical_apical/.../conf1_4.symm	apical, apical, conf1_2	$C_2$	-1709.617614 (2.2)	-1709.012236 (2.1)	-1709.113375 (3.8)
apical_apical/.../conf1_5	apical, apical, conf1_1	$C_1$	<b>-1709.621151 (0.0)</b>	<b>-1709.015523 (0.0)</b>	-1709.118781 (0.4)
apical_apical/.../conf2_1.symm	apical, apical, conf1_2	$C_2$	-1709.619438 (1.1)	-1709.014034 (0.9)	-1709.117115 (1.5)
apical_apical/.../conf2_3.symm	apical, apical, conf1_2	$C_2$	-1709.619939 (0.8)	-1709.014350 (0.7)	-1709.115157 (2.7)
apical_apical/.../conf2_5	apical, apical, conf1_2	$C_1$	-1709.620634 (0.3)	-1709.015211 (0.2)	<b>-1709.119426 (0.0)</b>

[a] For chiral structures, only one enantiomer is listed.

[b] Electronic energy.

**Figure S17.** UV-Vis spectra computed at the TD-M062X level for several conformers of the apical, apical isomer of model 2 (monocation, singlet).



## Part 4: Tetramethoxy-substituted compound

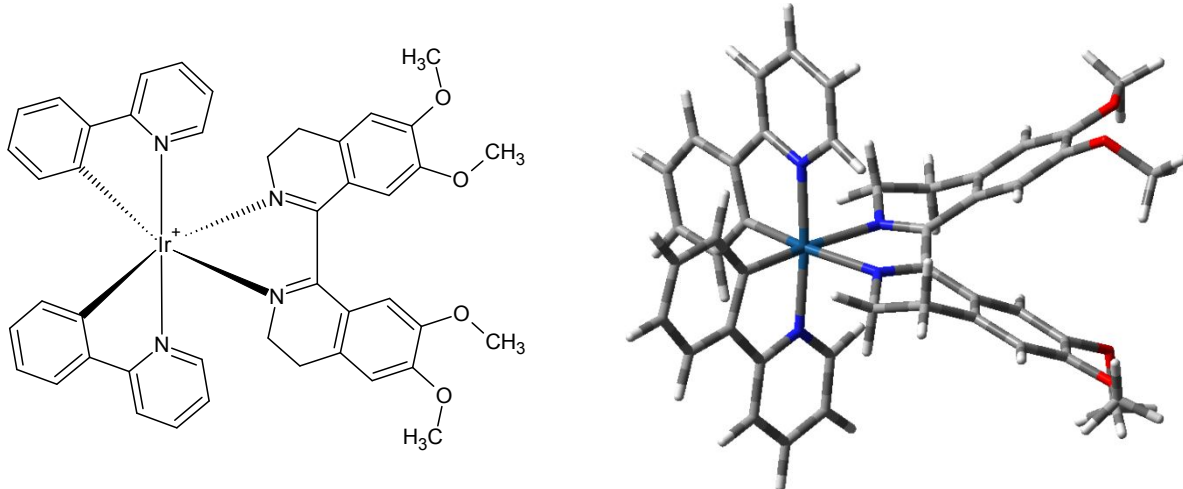


**Table S4.** Structural exploration of alternative isomers / conformers of the tetramethoxy-substituted compound (monocation, singlet). In parentheses relative energies (kcal mol<sup>-1</sup>) referred to the most stable form (in bold) identified at the specified level.

#	Isomer / Conformer <sup>a</sup>	Symmetry	<i>E</i> <sub>PCM</sub> / Ha <sup>b</sup>	<i>H</i> <sub>PCM,RRHO</sub> / Ha	<i>G</i> <sub>PCM,RRHO</sub> / Ha
apical_apical/.../conf1_5	apical, apical, conf1_5	<i>C</i> <sub>1</sub>	<b>-2324.022163</b> (0.0)	<b>-2323.216199</b> (0.0)	<b>-2323.343360</b> (0.0)
apical_apical/.../conf2_5	apical, apical, conf2_5	<i>C</i> <sub>1</sub>	-2324.019387 (1.7)	-2323.213914 (1.4)	-2323.342310 (0.7)
apical_equatorial/.../conf1_5	apical, equatorial, conf1_5	<i>C</i> <sub>1</sub>	-2324.019532 (1.7)	-2323.213177 (1.9)	-2323.339923 (2.2)
apical_equatorial/.../conf1_6	apical, equatorial, conf1_6	<i>C</i> <sub>1</sub>	-2324.019677 (1.6)	-2323.213547 (1.7)	-2323.342237 (0.7)
apical_equatorial/.../conf2_5	equatorial, equatorial, conf2_5	<i>C</i> <sub>1</sub>	-2324.018434 (2.3)	-2323.212823 (2.1)	-2323.340840 (1.6)
apical_equatorial/.../conf2_6	equatorial, equatorial, conf2_6	<i>C</i> <sub>1</sub>	-2324.018804 (2.1)	-2323.212947 (2.0)	-2323.339769 (2.3)

[a] For chiral structures, only one enantiomer is listed.

[b] Electronic energy.

**Table S5.** Computed [TD-M062X / 6-31+G(d,p) /PCM] high-wavelength ( $\lambda > 300$  nm) spin-allowed (singlet – singlet) electronic transitions in chloroform.

$\lambda/\text{nm}^a$	<i>f</i>	Contribution (expansion coefficient)	$\lambda/\text{nm}^a$	<i>f</i>	Contribution (expansion coefficient)	$\lambda/\text{nm}^a$	<i>f</i>	Contribution (expansion coefficient)
apical, apical, conf1_5			apical, apical, conf2_5			apical, equatorial, conf1_5		
404.4 [3.07]	0.00	190 → 191 (0.67)	406.2 [3.05]	0.00	190 → 191 (0.68)	407.1 [3.05]	0.03	179 → 191 (0.14) 185 → 191 (-0.11) 188 → 191 (0.10) 189 → 191 (0.12) 190 → 191 (0.63)
344.9	0.46	182 → 191 (-0.12) 184 → 191 (-0.10) 188 → 191 (-0.11) 189 → 191 (0.65) 190 → 193 (-0.11)	350.6	0.42	182 → 191 (0.11) 184 → 191 (-0.10) 188 → 191 (0.32) 189 → 191 (0.58)	379.3	0.10	180 → 191 (0.11) 181 → 191 (-0.14) 186 → 191 (0.14) 189 → 191 (0.63) 190 → 191 (-0.15)
340.6	0.08	183 → 191 (-0.27) 186 → 191 (-0.12) 187 → 191 (0.61)	348.0	0.11	183 → 191 (0.25) 187 → 191 (0.50) 188 → 191 (0.35) 189 → 191 (-0.17)	357.6	0.33	183 → 191 (0.15) 184 → 191 (-0.11) 188 → 191 (0.63) 190 → 191 (-0.12)
329.6	0.17	188 → 193 (-0.17) 190 → 191 (-0.11) 190 → 192 (0.64)	328.9	0.17	188 → 193 (-0.11) 189 → 193 (0.11) 190 → 192 (0.65)	326.4	0.16	185 → 191 (0.14) 187 → 191 (0.65)
318.7	0.05	188 → 191 (-0.12)	316.4	0.02	187 → 192 (0.13) 188 → 192 (-)	314.7	0.09	187 → 191 (-0.11)

		188 → 192 (-0.22) 189 → 191 (0.10) 190 → 193 (0.62)			0.16) 189 → 191 (0.14) 189 → 192 (0.16) 190 → 193 (0.61)			187 → 192 (-0.11) 187 → 193 (-0.10) 190 → 192 (0.47) 190 → 193 (0.43)
306.1	0.05	183 → 191 (0.53) 186 → 191 (0.24) 187 → 191 (0.28) 189 → 194 (-0.12)	307.9	0.07	183 → 191 (0.57) 186 → 191 (0.25) 187 → 191 (-0.19) 188 → 191 (-0.17)	304.9	0.17	189 → 192 (0.48) 189 → 193 (-0.32) 190 → 192 (0.24) 190 → 193 (-0.24)
			302.9	0.03	180 → 191 (0.26) 184 → 191 (0.19) 185 → 191 (0.11) 187 → 191 (-0.36) 188 → 191 (0.40) 189 → 191 (-0.18) 190 → 193 (0.16)			
<b>apical, equatorial, conf1_6</b>			<b>apical, equatorial, conf2_5</b>			<b>apical, equatorial, conf2_6</b>		
407.8 [3.04]	0.03	179 → 191 (-0.14) 185 → 191 (0.11) 188 → 191 (-0.12) 189 → 191 (-0.11) 190 → 191 (0.63)	403.0 [3.08]	0.06	179 → 191 (-0.14) 183 → 191 (0.11) 185 → 191 (0.12) 188 → 191 (-0.13) 190 → 191 (0.64)	403.1 [3.08]	0.07	179 → 191 (0.14) 183 → 191 (0.11) 185 → 191 (0.12) 188 → 191 (-0.12) 190 → 191 (0.64)
381.0	0.09	180 → 191 (0.11) 181 → 191 (0.13) 186 → 191 (0.15)	385.3	0.00	180 → 191 (0.12) 181 → 191 (0.15) 186 → 191 (-	384.9	0.00	180 → 191 (0.12) 181 → 191 (-0.16)

		189 → 191 (0.63) 190 → 191 (0.14)		0.14)	189 → 191 (0.64)			186 → 191 (-0.15) 189 → 191 (0.64)
360.4	0.32	183 → 191 (0.15) 184 → 191 (0.10) 188 → 191 (0.63) 190 → 191 (0.13)	368.1	0.40	183 → 191 (-0.16) 184 → 191 (-0.11) 188 → 191 (0.63) 190 → 191 (0.17)	365.8	0.41	183 → 191 (-0.16) 184 → 191 (-0.12) 188 → 191 (0.63) 190 → 191 (0.16)
325.4	0.17	185 → 191 (0.15) 187 → 191 (0.64) 190 → 192 (0.12)	329.6	0.13	185 → 191 (-0.11) 186 → 191 (0.15) 187 → 191 (0.65)	331.5	0.12	185 → 191 (-0.11) 186 → 191 (0.13) 187 → 191 (0.65)
315.0	0.10	187 → 191 (-0.13) 187 → 192 (0.12) 190 → 192 (0.51) 190 → 193 (-0.37)	312.1	0.10	190 → 192 (0.51) 190 → 193 (0.42)	312.4	0.11	187 → 192 (-0.11) 190 → 192 (0.54) 190 → 193 (-0.37)
304.2	0.17	189 → 192 (0.44) 189 → 193 (0.36) 190 → 192 (-0.22) 190 → 193 (-0.27)	303.5	0.14	183 → 191 (-0.18) 184 → 191 (-0.11) 189 → 192 (0.48) 189 → 193 (-0.35) 190 → 192 (-0.14) 190 → 193 (0.15)	302.7	0.14	183 → 191 (-0.17) 184 → 191 (-0.12) 189 → 192 (0.44) 189 → 193 (0.39) 190 → 192 (-0.14) 190 → 193 (-0.18)
			300.8	0.07	183 → 191 (0.39) 184 → 191 (0.37) 186 → 191 (-0.18)			

					188 → 191 (0.21) 188 → 194 (-0.11) 189 → 192 (0.18) 189 → 193 (-0.12)		
--	--	--	--	--	--	--	--

[a] In parentheses transition energies in eV.

[b] HOMO is MO #190.

**Table S6.** Computed [TD-M062X / 6-31+G(d,p) /PCM] high-wavelength ( $\lambda > 350$  nm) spin-forbidden (singlet – triplet) electronic transitions in chloroform.

$\lambda/\text{nm}^a$	Contribution (expansion coefficient)	$\lambda/\text{nm}^a$	Contribution (expansion coefficient)	$\lambda/\text{nm}^a$	Contribution (expansion coefficient)
apical, apical, conf1_5		apical, apical, conf2_5		apical, equatorial, conf1_5	
463.6 [2.67]	173 → 191 (-0.14) 174 → 191 (0.15) 187 → 191 (0.51) 189 → 194 (-0.22) 190 → 191 (0.27)	467.1 [2.65]	173 → 191 (-0.18) 174 → 191 (0.14) 179 → 191 (0.10) 183 → 191 (0.11) 187 → 191 (0.39) 188 → 191 (0.41) 189 → 194 (0.19)	491.0 [2.53]	173 → 191 (0.16) 179 → 191 (0.12) 183 → 191 (0.15) 187 → 191 (0.34) 188 → 191 (0.34) 188 → 194 (-0.16) 189 → 191 (0.11) 190 → 191 (0.34)
438.4	187 → 191 (0.10) 187 → 194 (-0.26) 188 → 191 (-0.12) 189 → 191 (0.59)	440.4	187 → 191 (-0.27) 187 → 194 (0.18) 188 → 191 (0.15) 188 → 194 (0.17) 189 → 191 (0.53)	465.6	187 → 191 (-0.12) 187 → 194 (-0.17) 188 → 191 (0.43) 188 → 194 (-0.11) 189 → 191 (0.23) 190 → 191 (-0.38)
410.7	173 → 191 (0.12) 187 → 191 (-0.22)	416.8	190 → 191 (0.64) 190 → 192 (0.13)	391.2	181 → 191 (-0.15) 185 → 191 (-0.12)

	188 → 193 (-0.14) 190 → 191 (0.53) 190 → 192 (0.26)				187 → 191 (-0.24) 189 → 191 (0.42) 190 → 191 (0.26) 190 → 192 (-0.17)
383.0	186 → 193 (-0.20) 188 → 192 (-0.39) 189 → 192 (-0.13) 190 → 193 (0.45)	382.9	186 → 192 (0.20) 187 → 193 (0.18) 188 → 193 (-0.20) 189 → 193 (0.20) 190 → 191 (-0.17) 190 → 192 (0.50)	384.0	186 → 191 (0.15) 187 → 191 (0.23) 187 → 193 (-0.10) 187 → 194 (0.13) 188 → 191 (-0.21) 189 → 191 (0.33) 189 → 192 (-0.13) 190 → 191 (-0.14) 190 → 192 (0.21) 190 → 193 (0.22)
381.2	186 → 192 (-0.20) 188 → 193 (-0.30) 189 → 193 (-0.11) 190 → 191 (-0.28) 190 → 192 (0.44)	381.6	186 → 193 (0.20) 187 → 192 (0.21) 188 → 192 (-0.25) 189 → 192 (0.24) 190 → 193 (0.45)	377.7	185 → 191 (-0.11) 185 → 192 (0.11) 187 → 191 (-0.25) 187 → 192 (-0.15) 187 → 193 (-0.12) 187 → 194 (-0.13) 188 → 191 (0.12) 190 → 191 (0.24) 190 → 192 (0.30) 190 → 193 (0.28)
				373.1	185 → 192 (-0.10) 186 → 192 (0.21) 186 → 193 (-0.19) 189 → 191 (-0.15) 189 → 192 (-0.35)

					189 → 193 (0.35) 190 → 192 (-0.16) 190 → 193 (0.14)
<b>apical, equatorial, conf1_6</b>		<b>apical, equatorial, conf2_5</b>		<b>apical, equatorial, conf2_6</b>	
492.9 [2.52]	173 → 191 (-0.16) 179 → 191 (0.11) 183 → 191 (0.16) 187 → 191 (0.29) 188 → 191 (0.41) 188 → 194 (0.16) 189 → 191 (0.10) 190 → 191 (-0.30)	494.4 [2.51]	173 → 191 (-0.16) 183 → 191 (-0.18) 187 → 191 (-0.30) 188 → 191 (0.47) 188 → 194 (-0.18) 190 → 191 (-0.19)	492.9 [2.52]	173 → 191 (-0.16) 179 → 191 (-0.11) 183 → 191 (-0.17) 187 → 191 (-0.34) 188 → 191 (0.41) 188 → 194 (-0.17) 190 → 191 (-0.24)
466.7	179 → 191 (-0.10) 187 → 191 (-0.19) 187 → 194 (0.16) 188 → 191 (0.38) 188 → 194 (0.11) 189 → 191 (0.21) 190 → 191 (0.42)	464.0	179 → 191 (-0.12) 187 → 191 (0.25) 187 → 194 (0.17) 188 → 191 (0.37) 189 → 191 (0.10) 190 → 191 (0.43)	464.6	179 → 191 (0.11) 187 → 191 (0.19) 187 → 194 (0.16) 188 → 191 (0.42) 190 → 191 (0.41)
392.6	181 → 191 (0.16) 187 → 191 (-0.20) 189 → 191 (0.46) 190 → 191 (-0.24) 190 → 192 (-0.16)	400.1	181 → 191 (0.12) 185 → 191 (-0.13) 187 → 191 (0.21) 187 → 194 (0.10) 189 → 191 (0.47) 190 → 191 (-0.32)	399.7	181 → 191 (-0.12) 185 → 191 (-0.12) 187 → 191 (0.22) 187 → 194 (0.10) 189 → 191 (0.45) 190 → 191 (-0.33) 190 → 192 (0.10)
384.7	185 → 191 (0.12) 186 → 191 (0.13) 187 → 191 (0.28)	388.9	181 → 191 (0.12) 186 → 191 (-0.17) 187 → 191 (-0.30)	388.6	181 → 191 (-0.12) 186 → 191 (-0.16) 187 → 191 (-0.29)

	187 → 194 (-0.15) 188 → 191 (-0.17) 189 → 191 (0.30) 189 → 192 (0.11) 190 → 191 (0.16) 190 → 192 (0.25) 190 → 193 (-0.20)		187 → 194 (-0.14) 188 → 191 (-0.12) 189 → 191 (0.38) 190 → 191 (0.24) 190 → 192 (-0.14) 190 → 193 (-0.15)		187 → 194 (-0.13) 188 → 191 (-0.12) 189 → 191 (0.40) 190 → 191 (0.22) 190 → 192 (-0.14) 190 → 193 (0.14)
377.8	185 → 191 (-0.12) 185 → 192 (-0.13) 186 → 192 (-0.11) 187 → 191 (-0.26) 187 → 192 (0.17) 187 → 193 (-0.10) 187 → 194 (0.13) 190 → 191 (-0.23) 190 → 192 (0.33) 190 → 193 (-0.25)	376.8	185 → 191 (0.11) 185 → 192 (-0.15) 185 → 193 (-0.12) 187 → 191 (-0.13) 187 → 192 (-0.16) 187 → 193 (-0.13) 190 → 191 (0.15) 190 → 192 (0.40) 190 → 193 (0.32)	377.0	185 → 191 (0.10) 185 → 192 (-0.17) 185 → 193 (0.11) 186 → 192 (0.10) 187 → 191 (-0.13) 187 → 192 (-0.17) 187 → 193 (0.12) 190 → 191 (0.14) 190 → 192 (0.43) 190 → 193 (-0.28)
372.8	186 → 192 (-0.19) 186 → 193 (-0.22) 189 → 191 (-0.12) 189 → 192 (0.31) 189 → 193 (0.39) 190 → 192 (-0.15) 190 → 193 (-0.17)	372.4	186 → 192 (-0.20) 186 → 193 (0.20) 189 → 192 (-0.38) 189 → 193 (0.39) 190 → 192 (0.10)	371.8	186 → 192 (0.19) 186 → 193 (0.22) 189 → 192 (0.34) 189 → 193 (0.42) 190 → 192 (-0.10) 190 → 193 (-0.13)

[a] In parentheses transition energies in eV.

[b] HOMO is MO #190.

**Table S7.** Structural exploration of alternative isomers / conformers of the tetramethoxy-substituted compound (monocation, triplet state). In parentheses relative energies (kcal mol<sup>-1</sup>) referred to the most stable form (in bold) identified at the specified level.

#	Isomer / Conformer <sup>a</sup>	Symmetry	<i>E</i> <sub>PCM</sub> / Ha <sup>b</sup>	<i>H</i> <sub>PCM,RRHO</sub> / Ha	<i>G</i> <sub>PCM,RRHO</sub> / Ha
apical_apical/.../TRIPLET/conf1_5	apical, apical, conf1_5	<i>C</i> <sub>1</sub>	- 2323.94481 2 (3.5)	- 2323.14032 4 (3.2)	- 2323.26938 1 (3.2)
apical_apical/.../TRIPLET/conf2_5	apical, apical, conf2_5	<i>C</i> <sub>1</sub>	- 2323.94291 3 (4.7)	- 2323.13875 9 (4.2)	- 2323.26870 6 (3.6)
apical_equatorial/.../TRIPLET/conf1_5	apical, equatorial, conf1_5	<i>C</i> <sub>1</sub>	- 2323.95032 7 (0.0)	- 2323.14541 6 (0.0)	- 2323.27373 3 (0.5)
apical_equatorial/.../TRIPLET/conf1_6	apical, equatorial, conf1_6	<i>C</i> <sub>1</sub>	- <b>2323.95034</b> <b>0 (0.0)</b>	- <b>2323.14548</b> <b>4 (0.0)</b>	- <b>2323.27447</b> <b>3 (0.0)</b>
apical_equatorial/.../TRIPLET/conf2_5	equatorial, equatorial, conf2_5	<i>C</i> <sub>1</sub>	- 2323.94656 8 (2.4)	- 2323.14250 6 (1.9)	- 2323.27167 5 (1.8)
apical_equatorial/.../TRIPLET/conf2_6	equatorial, equatorial, conf2_6	<i>C</i> <sub>1</sub>	- 2323.94687 0 (2.2)	- 2323.14303 6 (1.5)	- 2323.27243 8 (1.3)

[a] For chiral structures, only one enantiomer is listed.

[b] Electronic energy.

**Table S8.** Energies of alternative isomers / conformers of the tetramethoxy-substituted compound (monocation) computed in the first triplet state at the equilibrium geometry of the ground-state singlet. In parentheses relative energies (kcal mol<sup>-1</sup>) referred to the most stable form (in bold) identified at the specified level.

#	Isomer / Conformer <sup>a</sup>	Symmetry	<i>E</i> <sub>PCM</sub> / Ha <sup>b</sup>
apical_apical/.../TRIPLET_AT_SINGLET_GEOM_NONEQ_SOLV/conf1_5	apical, apical, conf1_5	<i>C</i> <sub>1</sub>	- 2323.92906 2 (0.6)
apical_apical/.../TRIPLET_AT_SINGLET_GEOM_NONEQ_SOLV/conf2_5	apical,	<i>C</i> <sub>1</sub>	-

	apical, conf2_5		2323.92769 9 (1.5)
apical_equatorial/.../TRIPLET_AT_SINGLET_GEOM_NONEQ_SOLV/conf1_5	apical, equatorial, conf1_5	$C_1$	- 2323.92945 6 (0.4)
apical_equatorial/.../TRIPLET_AT_SINGLET_GEOM_NONEQ_SOLV/conf1_6	apical, equatorial, conf1_6	$C_1$	- <b>2323.93006</b> <b>8 (0.0)</b>
apical_equatorial/.../TRIPLET_AT_SINGLET_GEOM_NONEQ_SOLV/conf2_5	equatorial, equatorial, conf2_5	$C_1$	- 2323.92857 3 (0.9)
apical_equatorial/.../TRIPLET_AT_SINGLET_GEOM_NONEQ_SOLV/conf2_6	equatorial, equatorial, conf2_6	$C_1$	- 2323.92911 8 (0.6)

[a] For chiral structures, only one enantiomer is listed.

[b] Electronic energy.

**Table S9.** Energies of alternative isomers / conformers of the tetramethoxy-substituted compound (monocation) computed for the ground-state singlet at the equilibrium geometry of the first triplet. In parentheses relative energies (kcal mol<sup>-1</sup>) referred to the most stable form (in bold) identified at the specified level.

#	Isomer / Conformer <sup>a</sup>	Symmetry	$E_{PCM}$ / Ha <sup>b</sup>
apical_apical/.../TRIPLET/SINGLET_AT_TRIPLET_GEOM_NONEQ_SOLV/conf1_5	apical, apical, conf1_5	$C_1$	- <b>2324.0050</b> <b>40 (0.0)</b>
apical_apical/.../TRIPLET/SINGLET_AT_TRIPLET_GEOM_NONEQ_SOLV/conf2_5	apical, apical, conf2_5	$C_1$	- 2324.0012 96 (2.3)
apical_equatorial/.../TRIPLET/SINGLET_AT_TRIPLET_GEOM_NONEQ_SOLV/conf1_5	apical, equatorial , conf1_5	$C_1$	- 2323.9937 74 (7.1)
apical_equatorial/.../TRIPLET/SINGLET_AT_TRIPLET_GEOM_NONEQ_SOLV/conf1_6	apical, equatorial , conf1_6	$C_1$	- 2323.9935 39 (7.2)
apical_equatorial/.../TRIPLET/SINGLET_AT_TRIPLET_GEOM_NONEQ_SOLV/conf2_5	equatorial , equatorial	$C_1$	- 2323.9951

	, conf2_5		77 (6.2)
apical_equatorial/.../TRIPLET/SINGLET_AT_TRIPLET_GEOM_NONEQ_SOL V/conf2_6	equatorial , equatorial , conf2_6	C <sub>1</sub>	- 2323.9961 34 (5.6)

[a] For chiral structures, only one enantiomer is listed.

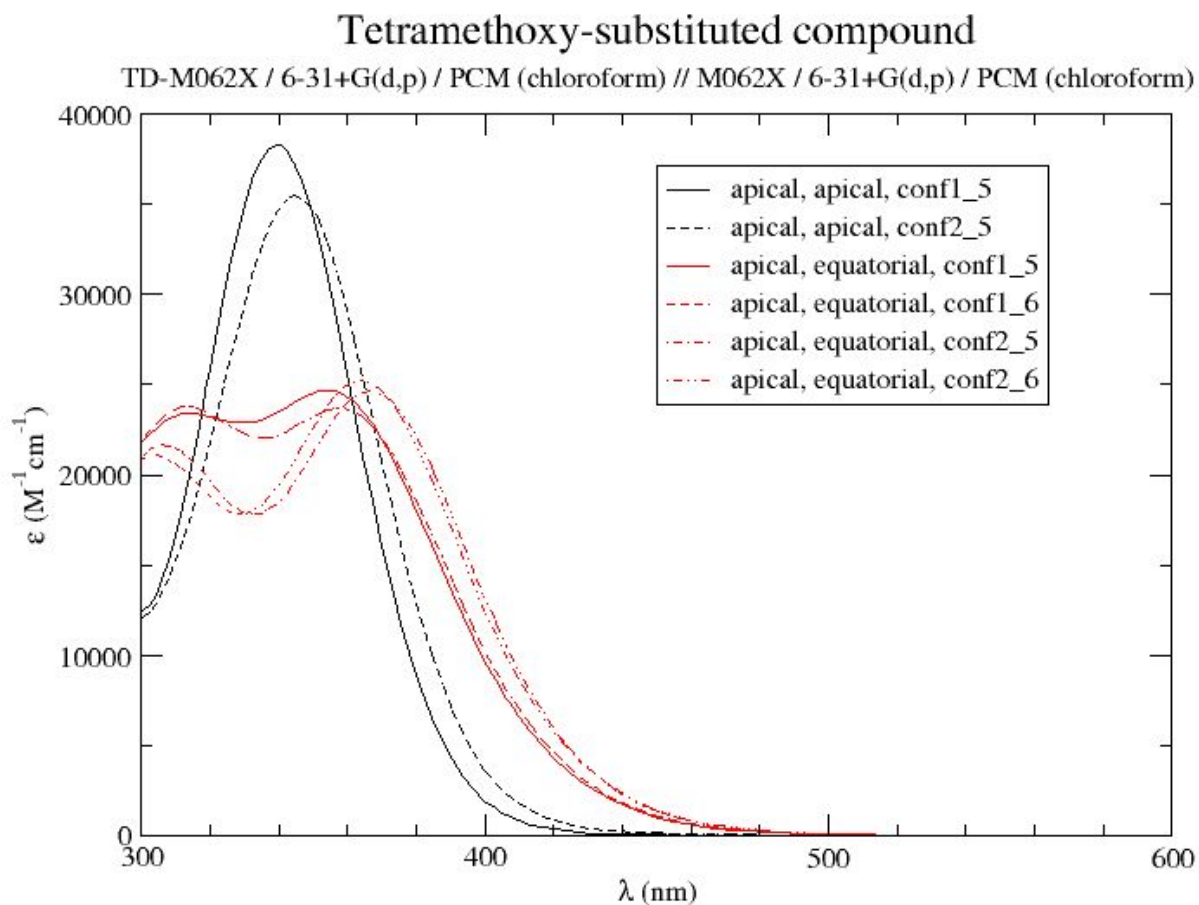
[b] Electronic energy.

**Table S10.** Summary of singlet and triplet energies of alternative isomers / conformers of the tetramethoxy-substituted compound (monocation). All energies (kcal mol<sup>-1</sup>) are referred to the most stable singlet.

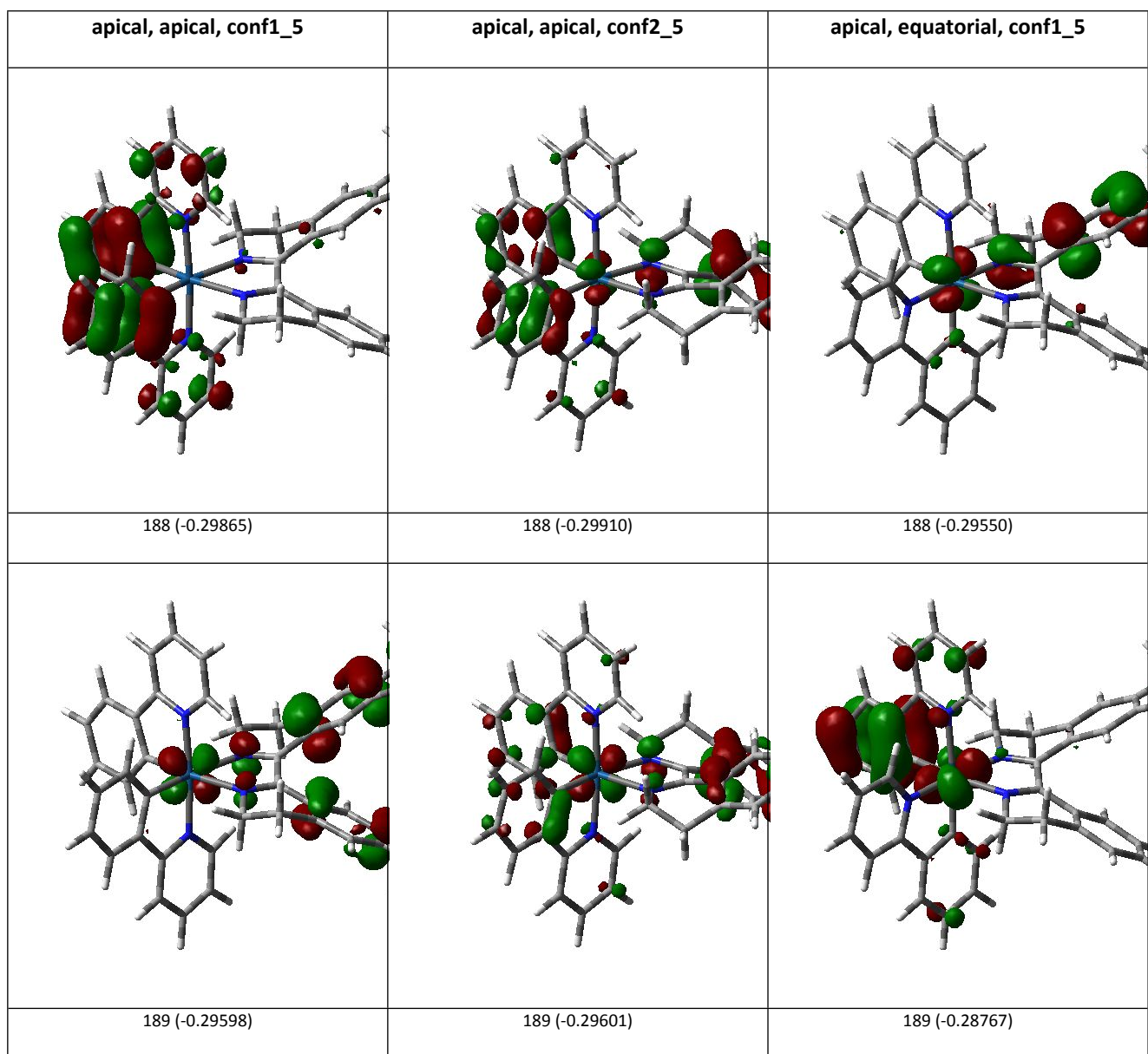
Isomer / Conformer <sup>a</sup>	Singlet / singlet geometry	Singlet / triplet geometry	Triplet / triplet geometry	Triplet / singlet geometry
apical, apical, conf1_5	<b>0.0</b>	10.7	48.5	58.4
apical, apical, conf2_5	1.7	13.1	49.7	59.3
apical, equatorial, conf1_5	1.7	17.8	45.1	58.2
apical, equatorial, conf1_6	1.6	18.0	45.1	57.8
equatorial, equatorial, conf2_5	2.3	16.9	47.4	58.7
equatorial, equatorial, conf2_6	2.1	16.3	47.2	58.4

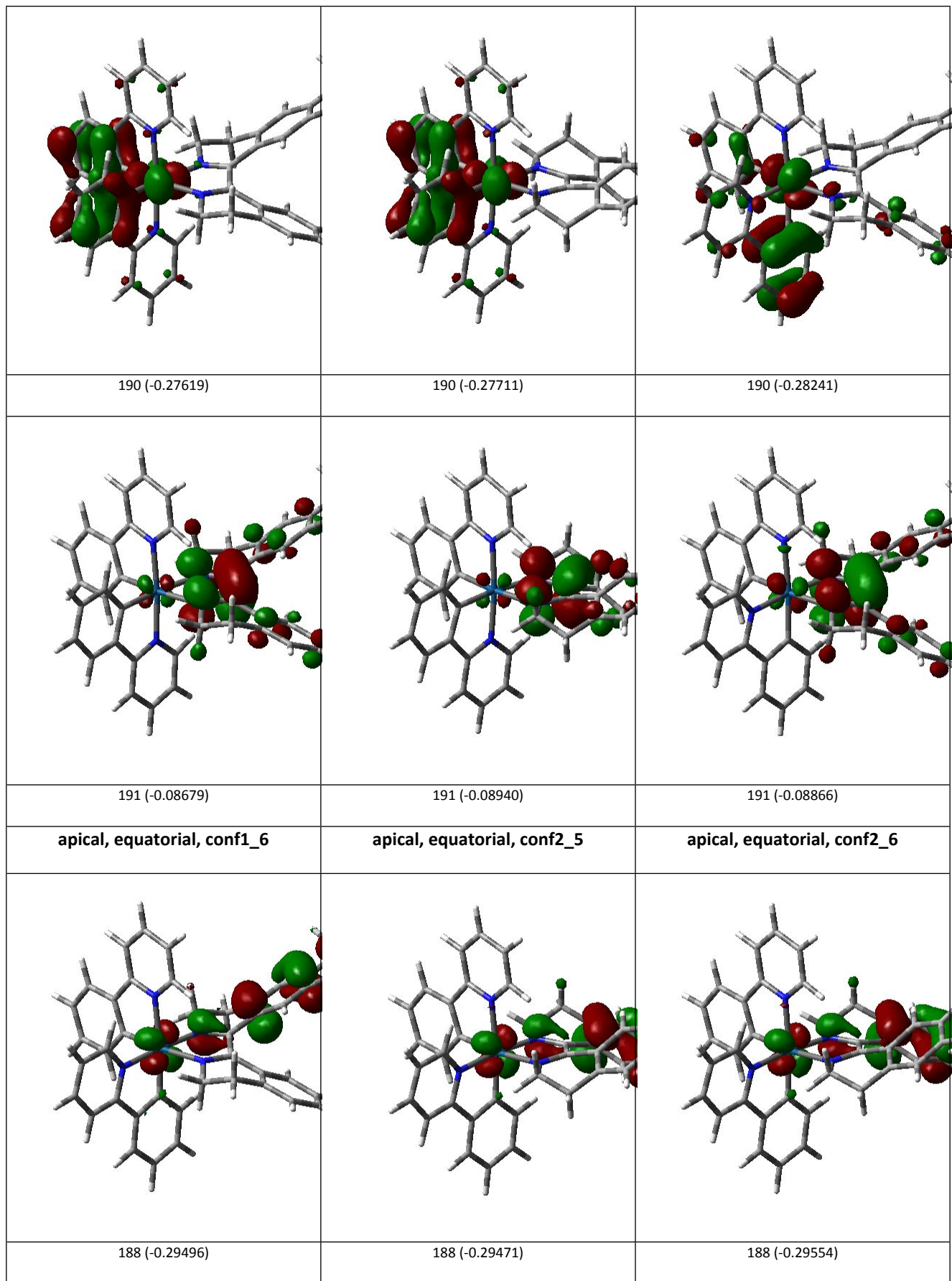
[a] For chiral structures, only one enantiomer is listed.

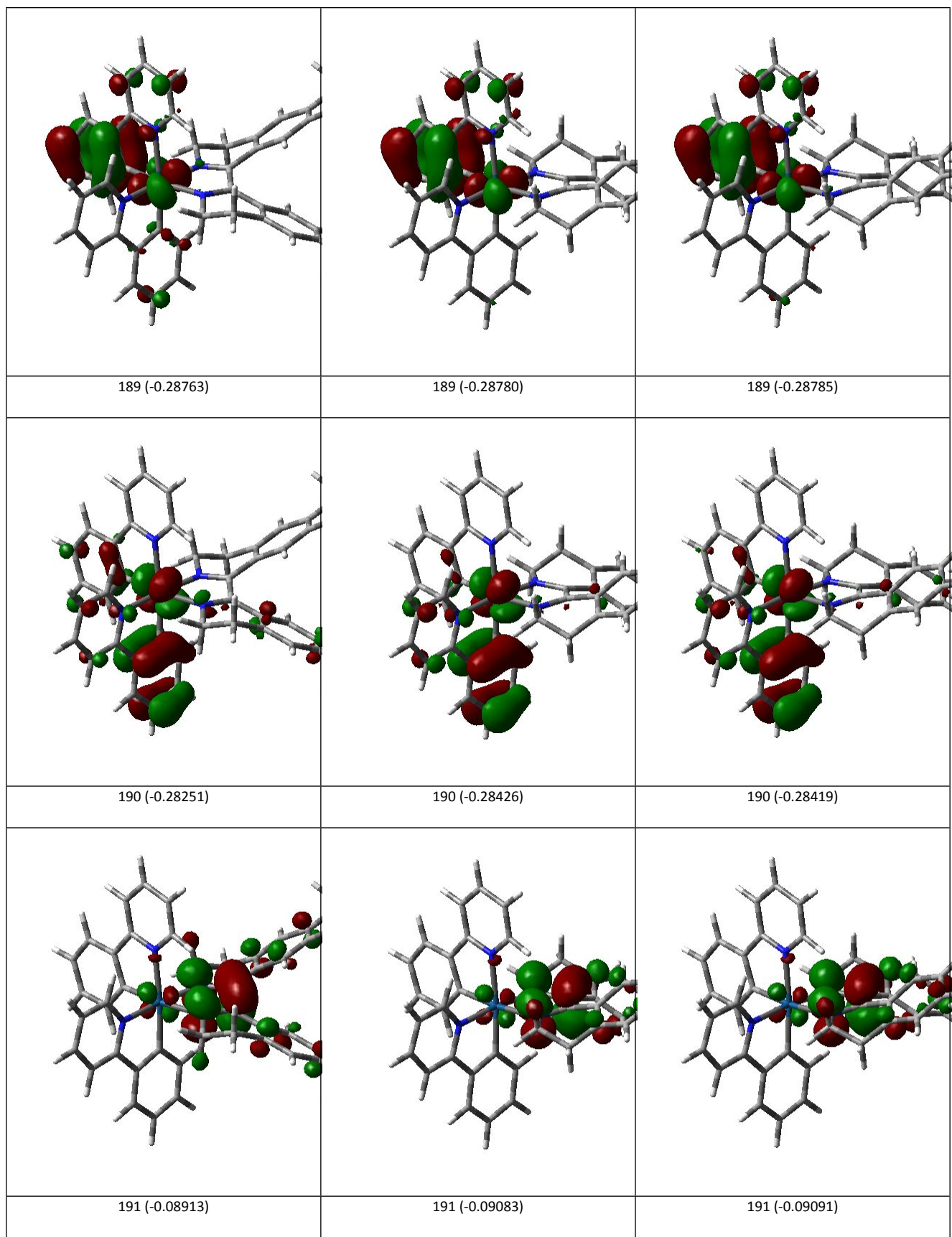
**Figure S18.** UV-Vis spectra computed at the TD-M062X level for several isomers / conformers of the tetramethoxy-substituted compound (monocation, singlet).



**Figure S19.** Selected molecular orbitals<sup>a</sup> [TD-M062X / 6-31+G(d,p) /PCM] in chloroform. Orbital energies (in hartree) are reported.

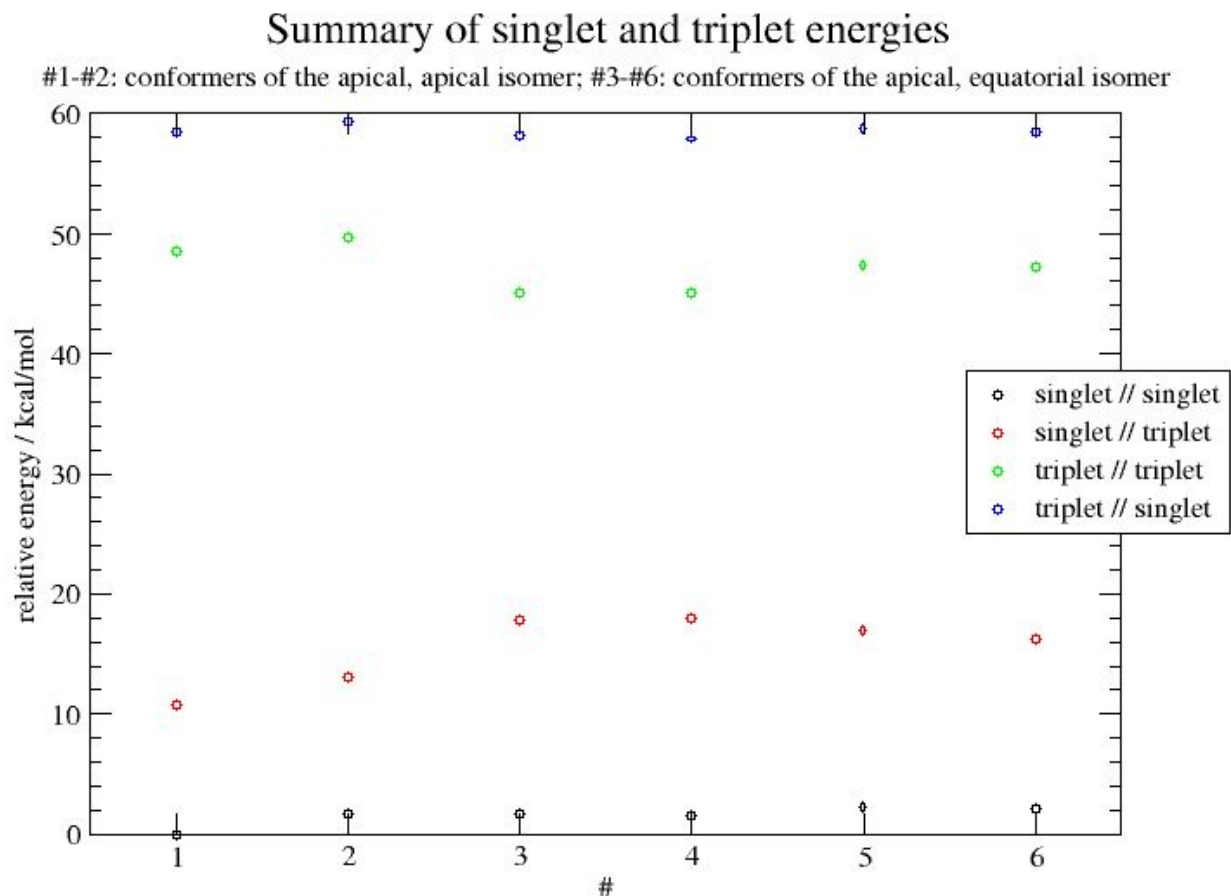






[a] Isodensity 0.04 a.u.

**Figure S20.** Summary of singlet and triplet energies of alternative isomers / conformers of the tetramethoxy-substituted compound (monocation). All energies ( $\text{kcal mol}^{-1}$ ) are referred to the most stable singlet.



## References

- 1) Manini, P.; Panzella, L.; Tedesco, I.; Petitto, F.; Russo, G. L.; Napolitano, A.; Palumbo, A.; d'Ischia, M. Tetrahydrobisoquinoline Derivatives by Reaction of Dopamine with Glyoxal: A Novel Potential Degenerative Pathway of Catecholamines under Oxidative Stress Conditions. *Chem. Res. Toxicol.* **2004**, *17*, 1190-1198.
- 2) Nonoyama, M. Benzo[h]quinolin-10-yl-N Iridium(III) Complexes. *Bull. Chem. Soc. Jpn.*, **1974**, *47*, 767-768.
- 3) Frisch, M. J.; Trucks, G. W.; Schlegel, H. B.; Scuseria, G. E.; Robb, M. A.; Cheeseman, J. R.; Scalmani, G.; Barone, V.; Mennucci, B.; Petersson, G. A.; Nakatsuji, H.; Caricato, M.; Li, X.; Hratchian, H. P.; Izmaylov, A. F.; Bloino, J.; Zheng, G.; Sonnenberg, J. L.; Hada, M.; Ehara, M.; Toyota, K.; Fukuda, R.; Hasegawa, J.; Ishida, M.; Nakajima, T.; Honda, Y.; Kitao, O.; Nakai, H.; Vreven, T.; Jr Montgomery, J. A.; Peralta, J. E.; Ogliaro, F.; Bearpark, M.; Heyd, J. J.; Brothers, E.; Kudin, K. N.; Staroverov, V. N.; Keith, T.; Kobayashi, R.; Normand, J.; Raghavachari, K.; Rendell, A.; Burant, J. C.; Iyengar, S. S.; Tomasi, J.; Cossi, M.; Rega, N.; Millam, J. M.; Klene, M.; Knox, J. E.; Cross, J. B.; Bakken, V.; Adamo, C.; Jaramillo, J.; Gomperts, R.; Stratmann, R. E.; Yazyev, O.; Austin, A. J.; Cammi, R.; Pomelli, C.; Ochterski, J. W.; Martin, R. L.; Morokuma, K.; Zakrzewski, V. G.; Voth, G. A.; Salvador, P.; Dannenberg, J. J.; Dapprich, S.; Daniels, A. D.; Farkas, Ö.; Foresman, J. B.; Ortiz, J. V.; Cioslowski, J.; Fox, D. J. *Gaussian 09*, Revision D.01, Gaussian, Inc., Wallingford CT, **2013**.
- 4) Zhao, Y.; Truhlar, D. G. The Mo6 suite of density functionals for main group thermochemistry, thermochemical, kinetics, noncovalent interactions, excited states, and transition elements: two new functionals and systematic testing of four Mo6-class functionals and 12 other functionals. *Theor. Chem. Acc.* **2008**, *120*, 215-241.

- 5) Dolg, M.; Wedig, U.; Stoll, H.; Preuss, H. Energy-adjusted ab initio pseudopotentials for the first row transition elements. *J. Chem. Phys.* **1987**, *86*, 866-872.
- 6) Andrae, D.; Haeussermann, U.; Dolg, M.; Stoll, H.; Preuss, H. Energy-adjusted *ab initio* pseudopotentials for the second and third row transition elements. *Theor. Chim. Acta* **1990**, *77*, 123-141.
- 7) Miertus, S.; Scrocco, E.; Tomasi, J. Electrostatic interaction of a solute with a continuum. A direct utilization of AB initio molecular potentials for the prevision of solvent effects. *J. Chem. Phys.* **1981**, *55*, 117-129.
- 8) Cossi, M.; Scalmani, G.; Rega, N.; Barone, V. New developments in the polarizable continuum model for quantum mechanical and classical calculations on molecules in solution. *J. Chem. Phys.* **2002**, *117*, 43-54.
- 9) Scalmani, G.; Barone, V.; Kudin, K. N.; Pomelli, C. S.; Scuseria, G. E.; Frisch, M. J. Achieving linear-scaling computational cost for the polarizable continuum model of solvation. *Theor. Chem. Acc.* **2004**, *111*, 90-100.
- 10) Tomasi, J.; Mennucci, B.; Cammi, R. Quantum Mechanical Continuum Solvation Models. *Chem. Rev.* **2005**, *105*, 2999-3093.
- 11) Rappé, A. K.; Cesewit, C. J.; Colwell, K. S.; Goddard, W. A. III.; Skiff, W. M. UFF, a full periodic table force field for molecular mechanics and molecular dynamics simulations. *J. Am. Chem. Soc.* **1992**, *114*, 10024-10035.
- 12) York, D. A.; Karplus, M. A Smooth Solvation Potential Based on the Conductor-Like Screening Model. *J. Phys. Chem. A.* **1999**, *103*, 11060-11079.
- 13) Scalmani, G.; Frisch, M. J. Continuous surface charge polarizable continuum models of solvation. I. General formalism. *J. Chem. Phys.* **2010**, *132*, 114110.
- 14) Stratmann, R. E.; Scuseria, G. E.; Frisch, M. J. An efficient implementation of time-dependent density-functional theory for the calculation of excitation energies of large molecules. *J. Chem. Phys.* **1998**, *109*, 8218-8224.

- 15) Bauernschmitt, R.; Ahlrichs, R. Treatment of electronic excitations within the adiabatic approximation of time dependent density functional theory. *Chem. Phys. Lett.* **1996**, *256*, 454-464.
- 16) Casida, M. E.; Jamorski, C.; Casida, K. C.; Salahub, D. R. Molecular excitation energies to high-lying bound states from time-dependent density-functional response theory: Characterization and correction of the time-dependent local density approximation ionization threshold. *J. Chem. Phys.* **1998**, *108*, 4439-4449.
- 17) Adamo, C.; Scuseria, G. E.; Barone, V. Accurate excitation energies from time-dependent density functional theory: Assessing the PBE0 model. *J. Chem. Phys.* **1999**, *111*, 2889-2899.
- 18) Scalmani, G.; Frisch, M. J.; Mennucci, B.; Tomasi, J.; Cammi, R.; Barone, V. Geometries and properties of excited states in the gas phase and in solution: Theory and application of a time-dependent density functional theory polarizable continuum model. *J. Chem. Phys.* **2006**, *124*, 094107.
- 19) Adamo, C.; Barone, V. Toward reliable density functional methods without adjustable parameters: The PBE0 model. *J. Chem. Phys.* **1999**, *110*, 6158-6169.
- 20) Yanai, T.; Tew, D.; Handy, N. A new hybrid exchange?correlation functional using the Coulomb-attenuating method (CAM-B3LYP). *Chem. Phys. Lett.* **2004**, *393*, 51-57.
- 21) Vydrov, O. A.; Scuseria, G. E. Assessment of a long-range corrected hybrid functional. *J. Chem. Phys.* **2006**, *125*, 234109.
- 22) Improta, R.; Barone, V.; Scalmani, G.; Frisch, M. J. A state-specific polarizable continuum model time dependent density functional theory method for excited state calculations in solution. *J. Chem. Phys.* **2006**, *125*, 054103.
- 23) Improta, R.; Scalmani, G.; Frisch, M. J.; Barone, V. Toward effective and reliable fluorescence energies in solution by a new state specific polarizable continuum model time dependent density functional theory approach. *J. Chem. Phys.* **2007**, *127*, 074504.